

1 Exo-GPU: Safe, Imperative, User-schedulable Programming 2 for Tensor Cores

3 ANONYMOUS AUTHOR(S)

4 Modern GPUs require not only SIMD-style parallelism but also software-managed concurrency between
5 compute and data movement to reach maximum performance. Performance engineers must reason about
6 subdividing work into the hierarchy of computation resources (threads, warps, warpgroups, blocks, clusters),
7 and, in many cases, also must use asynchronous tensor core and memcpy instructions on different levels
8 of the memory hierarchy (registers, tensor core accumulators, shared memory, global memory). Unlike
9 CPUs, where out-of-order execution is managed by hardware and hidden from programmers, GPUs expose
10 explicit instruction reordering to software through these asynchronous instructions. Well-established GPU
11 programming languages generally offer either direct low-level control without safety guarantees (e.g., CUDA
12 C++ inline assembly or intrinsics) or easier-to-analyze, high-level abstractions (e.g., Triton’s tile-based model)
13 that hide asynchronous instructions in the compiler backend, which may prevent performance engineers from
14 maximizing performance by tuning critical details.

15 We propose Exo-GPU, an imperative, low-level language that creates minimal abstraction over CUDA. Our
16 key idea is to treat parallelism and synchronization as mere annotations on sequential code rather than as
17 fundamental control flow primitives, enabling verification that these constructs do not alter the program
18 semantics. The benefit is two-fold: programmers can reason about code without hidden control flow or
19 mutation, while allowing the Exo-GPU compiler to verify *sequential-parallel equivalence*—guaranteeing that
20 parallel execution is functionally equivalent to its sequential interpretation. We used Exo-GPU to author GEMM
21 kernels for the H100 GPU, using wmma, TMA, and split-k. Our kernels achieved over 80% of theoretical peak
22 on large problem sizes, in some cases outperforming the vendor-provided CUBLAS library.

23 1 INTRODUCTION

24 Starting with Tensor Cores introduced in NVIDIA’s Volta generation of GPUs [13], the menu of
25 tensor-specialized features in NVIDIA GPUs has expanded to encompass automated bulk move-
26 ment of multidimensional data, distributed shared memory, and new asynchronous tensor cores
27 supporting large-scale (up to 64×256) matrix accumulation in a single instruction [18]. This
28 poses ever-increasing challenges for authoring correct, top-performing CUDA code. Not only must
29 algorithms be rewritten to migrate work from traditional SIMD-style code to target these specialized
30 instructions, but also, these instructions expose explicit out-of-order instruction execution to the
31 programmer, moving synchronization that was traditionally the responsibility of the hardware
32 (e.g., through scoreboarding) to the programmer.

33 High-level kernel programming languages, such as Triton [24], provide a popular approach for
34 taming this complexity. Triton’s tile-based, automatically-parallelized programming model reduces
35 the risk of programmer error by moving responsibility for correct usage of bulk data movement and
36 synchronization instructions into the compiler. However, in practice, groundbreaking algorithms,
37 such as the original FlashAttention 3 [21], are often written directly in CUDA C++ for greater
38 control. On the one hand, CUDA C++ provides direct control over features such as asynchronous
39 data movement and warp specialization required for optimal GPU usage. On the other hand, CUDA
40 C++ exposes programmers to a variety of potential bugs, which we broadly categorize as:

- 41 (1) *Dataflow Logic Bugs*: Program optimization usually requires changing the storage or com-
42 putation order of intermediate values, e.g. caching data in a faster memory, or reordering
43 instructions to hide latency. A flawed optimization, such as an indexing bug in copying a
44 tile, or exchanging two statements that don’t commute safely, can change the functional
45 behavior of the program.
- 46 (2) *Instruction Logic Bugs*: Accelerator instructions won’t work as intended if not used as
47 specified by the hardware vendor. For example, wmma tensor core instructions require data
48 in a certain input format and uniform execution by a full warpgroup (128 aligned threads).

- 50 (3) *Inter-Thread Synchronization Bugs*: Garden-varietiy synchronization bugs involve two threads
 51 accessing the same memory location (with one access being a write) without ordering
 52 enforced by synchronization.
 53 (4) *Intra-Thread Synchronization Bugs*: If one thread issues an asynchronous (async) instruction,
 54 and that *same thread* later issues another instruction (async or not) that operates on the same
 55 memory location, overlapped or reordered instruction execution can undermine correctness.

56 Our goal is to provide a programming model that gives CUDA-like control *without* accepting the
 57 risk of these bugs as a fact of life. Existing CUDA C++ libraries such as CuTe [14] and ThunderKittens
 58 [22] provide close-to-the-metal abstractions that minimize the risk of logic bugs, particularly data
 59 movement and instruction input format bugs; however, none of them support large-scale program
 60 analysis and synchronization checking of arbitrary input programs.

61 As a starting point for the Exo-GPU language design, we postulate that programs with *sequential*
 62 *semantics* are far easier to analyze, both by humans and by compilers. We define program behavior
 63 using standard sequential semantics, treating language features for parallelism and synchronization—
 64 including parallel for-loops across CUDA thread hierarchies and barrier statements—simply as
 65 *annotations* on sequential code. This design provides two key benefits: programmers can intuitively
 66 reason about their code without hidden control flow or side effects, and more importantly, compilers
 67 can verify whether synchronizations are legal; that is, they can verify these annotations do not
 68 alter the program behavior relative to its baseline sequential interpretation.

69 The Exo-GPU program, interpreted sequentially, serves as the semantic baseline—defining
 70 *what* the user intends to compute. Parallelism annotations specify *which threads* execute which
 71 statement instances, while synchronization constructs specify *how* the user intends to uphold
 72 baseline behavior. This raises a question: what degree of safety and control does Exo-GPU provide?
 73 We define safety as *sequential-parallel equivalence*—ensuring that the parallel interpretation of
 74 a program matches the sequential one. Parallelism is explicitly controlled by the programmer’s
 75 annotations, rather than being hidden and automated by the compiler. The Exo-GPU compiler’s
 76 role is limited to *verifying* that the user-provided synchronization ensures equivalence.

77 Through collective analysis (Section 4), we annotate each statement with a *collective tiling*,
 78 specifying which thread(s) execute each statement instance. This enables static analysis of the
 79 thread assignment counts, ensuring instructions with thread convergence requirements (e.g. warp
 80 MMA) are used correctly. To ensure sequential-parallel equivalence, we simulate execution on an
 81 *abstract machine* (Section 5). The Exo-GPU program converts to an Abstract Machine program
 82 where data variables store access histories (reads and mutations) with their thread and sync
 83 instruction *visibility*, rather than numeric values. Synchronization statements become meaningful
 84 only in the abstract machine, conditionally expanding the visibility of all prior recorded accesses.

85 We built Exo-GPU as an extension to Exo [7, 8], a user-schedulable language providing com-
 86 posable, checked rewrite rules for transforming sequential programs. Exo lacks GPU support, and
 87 we significantly extended its frontend language design, static analysis, semantics, and codegen to
 88 enable safe parallel program transformation. Treating parallel constructs as annotations over a
 89 sequential semantic baseline enabled us to reuse Exo’s over 60 verified rewrites as-is, which allowed
 90 us to transform a simple sequential GEMM program into a complex GEMM kernel for the NVIDIA
 91 Hopper architecture, with every step of transformation verified via a *chain of equivalence*: Exo
 92 verified equivalence between the original p_1 and the final p_n while ignoring all the synchronization
 93 constructs, and Exo-GPU verified functional equivalence between the parallel and sequential inter-
 94 pretations of p_n , checking the legality of the parallel and synchronous annotations (Section 2.3).
 95 Combining Exo’s pre-existing checked rewrite rules with Exo-GPU’s new language features and
 96 synchronization checking, we created a GEMM kernel achieving over 80% of theoretical peak for
 97 large problem sizes, in some cases outperforming the vendor-supplied CUBLAS library (Section 6).

99 2 EXAMPLES AND SYSTEM OVERVIEW

100 2.1 Exo-GPU Language Overview

101 Exo-GPU is built on fundamental design goals of safe, performance transparent, and imperative
 102 GPU programming. Unlike other GPU abstractions that hide complexity, we make threads and most
 103 CUDA instructions explicit in the IR. We introduce three first-class frontend language features de-
 104 rived from our design principles: (i) parallel loops that explicitly map work to blocks/warps/threads,
 105 (ii) a distributed memory model with sharding and explicit memory space annotations, and (iii)
 106 explicit synchronization, including fences, split-barriers, and asynchronous operations.
 107

108 **Parallel loops.** Exo-GPU exposes three kinds of loops. (1) $\text{seq}(c_{lo}, c_{hi})$ is a sequential loop that
 109 iterates i from c_{lo} to $c_{hi}-1$. (2) $\text{cuda_tasks}(lo, hi)$ distributes iterations across CUDA clusters; on pre-
 110 sm_90 (H100) GPUs a cluster coincides with a single CTA (thread block). (3) $\text{cuda_threads}(lo, hi, \text{unit} =$
 111 τ_u) assigns iterations to subsets of threads inside the current cluster. The unit takes a parameter
 112 τ_u that specifies the shape of the participating thread set but not concrete indices—for example,
 113 $\tau_u = \text{cuda_warp}$ denotes contiguous 32-thread groups with thread IDs 0–31, 32–63, 64–95, etc.
 114 (inclusive), while $\tau_u = \text{cuda_thread}$ denotes a single thread (see Figure 11).

115 Each loop body, conditional branch, with-block, or proce-
 116 dure defines a *program scope*. As part of *collective analysis* (Sec-
 117 tion 4), we annotate each scope with a *collective tiling* $\omega \in \Omega$.
 118 This describes a mapping between the control variable values
 119 and the *thread collective* (set of threads) assigned to execute
 120 statement instances in the scope (i.e. which threads execute
 121 which loop iterations). We say that a scope is a τ_u -scope when
 122 τ_u accurately describes the thread sets produced by the mapping. In the inset figure, the out-
 123 ermost parallel loop $\text{cuda_tasks}(0, 37)$ creates scope-1 (which is a cluster scope, and, assum-
 124 ing $\text{clusterDim}=1$, also a CTA scope); nesting $\text{cuda_threads}(\dots, \text{unit}=\text{cuda_warp})$ creates
 125 scope-2 (warp scope); and nesting $\text{cuda_threads}(\dots, \text{unit}=\text{cuda_thread})$ creates scope-3
 126 (single-thread scope). Statement instances in scope-3 are executed by one thread.

127 **Distributed Memory:** Exo-GPU exposes explicit allocation statements for data and barrier
 128 variables, annotated by memory type, e.g. $x : \text{f32}[8] @ \text{CudaRmem}$ allocates a data array x
 129 of type f32 and size 8 in GPU register memory. Allocations can be *distributed*: a single logical
 130 object may be sharded across threads at multiple CUDA levels (e.g., per-thread register shards or
 131 per-CTA-in-cluster shared-memory shards). Threads must access only their owned shards except
 132 via explicit communication instructions (e.g., warp shuffles) or TMA multicast. This sharding is
 133 not annotated explicitly at the allocation, but deduced from the usage pattern of the variable; all
 134 deductions must be consistent, as enforced by distributed memory analysis (Section 4.1).

135 Inset right illustrates the motivation for this design. If the
 136 first loop was executed sequentially, tmp would hold $A[31]$
 137 after the first loop, so the second loop broadcasts that value
 138 to every $B[i]$. Languages like CUDA that implicitly duplicate
 139 local variables per thread would interpret the same code as a
 140 vector copy ($B[i] = A[i]$). While not necessarily error-prone,
 141 this design would be inappropriate for our goal of defining program behavior with sequential
 142 semantics. Hence, in Exo-GPU, storing a temporary value per-thread requires a sharded allocation
 143 of tmp ; as written, the program is rejected by the analysis because a register-resident tmp cannot
 144 be read by different threads without (for example) a warp shuffle. If a user intends to express a
 145 vector copy ($B[i] = A[i]$) through register tmp , tmp requires explicit *distributed* allocation per
 146 thread ($\text{tmp} : \text{f32}[32]$) and the accesses must be per-thread ($\text{tmp}[i]$).

```
for blk in cuda_tasks(0, 37):
    # scope-1 (CTA-scope)
    for w in cuda_threads(0, 4,
                           unit=cuda_warp):
        # scope-2 (warp-scope)
        for t in cuda_threads(0, 32,
                           unit=cuda_thread):
            # scope-3 (thread-scope)
```

```
tmp: f32 @ CudaRmem # Register
for i in cuda_threads(0, 32,
                      unit=cuda_thread):
    tmp = A[i]
for i in cuda_threads(0, 32,
                      unit=cuda_thread):
    B[i] = tmp
```

148 **Explicit Synchronization:** Many GPU instructions require additional explicit synchronization,
 149 but overly conservative barriers can cancel the performance benefits of concurrency. Exo-GPU
 150 provides two forms of synchronization: a blocking barrier via Fence, and split barriers via paired
 151 Arrive/Await. As with other statements, all synchronization statements execute in program order.

152 A Fence causes all threads in the current
 153 thread collective (warp, CTA, or cluster) to ren-
 154 dezvous. At warp scope it maps to `__syncwarp`;
 155 at CTA scope it maps to `__syncthreads` (as
 156 shown in the right-hand code inset). A Fence
 157 takes two synchronization-timeline parame-
 158 ters, τ_s^{pre} and τ_s^{post} (Figure 16). These timelines
 159 specify which memory operations (sync and/or
 160 async) before and after the fence must be or-
 161 dered, and the compiler emits the minimal
 162 combination of synchronization and memory-fence instructions required to satisfy them. The
 163 `cuda_in_order` timeline specifies that the effects of async instructions are *not* synchronized, but
 164 only regular synchronous instructions. If we were to, for example, replace the loads into shared
 165 memory with `cp.async` operations, the first parameter must be set to `Sm80_cp_async` so that the
 166 copy operations preceding the fence are completed before execution proceeds.

167 Split barriers use a shared barrier-typed variable z , declared
 168 as $z: \text{barrier} @ \pi_b$, where π_b selects the completion mecha-
 169 nism (commit group, mbarrier, or cluster sync). Programmers
 170 express a split barrier statement pair with $\text{Arrive}(\tau_s^{\text{pre}}) \gg z$
 171 and $\text{Await}(z, \tau_s^{\text{post}})$. The statement pairing is determined by
 172 the shared barrier variable z . A matching pair orders memory op-
 173 erations prior to `Arrive` (filtered by τ_s^{pre}) with those after `Await`
 174 (filtered by τ_s^{post}). The right-hand inset illustrates replacing the
 175 earlier Fence example with an `mbarrier`-based split barrier.

```
# Code at CTA-scope, with blockDim=128
buf: f32[128] @ CudaSmemLinear
for tid in cuda_threads(0, 128, unit=cuda_thread):
    buf[tid] = gmem[tid]
# __syncthreads
Fence(cuda_in_order, cuda_in_order)
for tid in cuda_threads(0, 128, unit=cuda_thread):
    accum: f32 # Each thread sums up buf[...]
    accum = 0
    for i in seq(0, 128):
        accum += buf[i]
```

```
for tid in cuda_threads(0, 128,
                       unit=cuda_thread):
    ...
bar: barrier @ CudaMbarrier
Arrive(cuda_in_order) >> bar
# ... insert work here
Await(bar, cuda_in_order)
for tid in cuda_threads(0, 128,
                       unit=cuda_thread):
    ...
```

177 2.2 Exo-GPU Examples with Erroneous Synchronization

178 To motivate our language design, we build up a series of increasingly subtle, hard-to-identify inter-
 179 and intra-thread synchronization bugs; all would be rejected by synchronization checking (Sec-
 180 tion 5). Variables prefixed with `some_*` are allocated outside the code snippet, `some_in_order_op`
 181 represents non-async work, and `example_tma_multicast` and `example_wgmma` are simplified place-
 182 holders for actual TMA (tile copy) and wgmma (tensor core) instructions.

183 The first example illustrates an inter-thread synchronization bug involving a cluster with 2 CTAs:

```
B: f32[2, 256, 32] @ CudaSmemLinear # Distributed mem: B[0,:,:] on CTA 0; B[1,:,:] on CTA 1
for cta in cuda_threads(0, 2, unit=cuda_cta_in_cluster):
    some_in_order_op(B[cta, :, :])
    Fence(cuda_in_order, cuda_in_order) # __syncthreads
example_tma_multicast(B[:, :, :], some_gmem[:, :, :]) # Copy some_gmem[:, :] to B[0,:,:] and B[1,:,:]
```

189 The `example_tma_multicast` instruction is implemented by threads in the 2 CTAs cooperating to
 190 fill each others' shared memory; however, this cooperation does not entail implicit synchronization
 191 between the two CTAs. Since the `Fence` statement, as placed in CTA-scope, only synchronizes
 192 threads within a CTA, it is possible that threads in CTA 0 proceed to the multicast instruction,
 193 filling the SMEM of CTA 1 (`B[1, :, :]`), while threads in CTA 1 are still reading from it while
 194 executing `some_in_order_op`. Although the TMA instruction is async, this is not relevant to the
 195 bug illustrated here, as the TMA appears after the in-order operations upon which it races with.

197 The next example illustrates an intra-thread synchronization bug:

```
198 D: f32[2, 2, 64, 256] @ Sm90_RmemMatrixD(64, 256) # Distributed: D[x,y,:,:] on CTA x, warpgroup y
199 for cta in cuda_threads(0, 2, unit=cta_in_cluster):
200     for wg in cuda_threads(0, 2, unit=cuda_warpgroup):
201         example_wgmma(D[cta, wg, :, :], some_A[:, :], some_B[:, :]) # D += matmul(A, B)
202         some_in_order_op(D[cta, wg, :, :])
```

203 This code parallelizes across CTAs and warpgroups, with each warpgroup accessing only its own
 204 shard D[cta, wg, :, :]. Nevertheless, the code is flawed, as the async example_wgmma instruction
 205 isn't waited-for before some_in_order_op attempts to access its output.

206 A more subtle bug arises when async instructions interact with inter-thread synchronization:

```
207 B: f32[2, 256, 32] @ Sm90_SmemSwizzled(128) # Distributed: B[x,:,:] on CTA x
208 D: f32[2, 2, 64, 256] @ Sm90_RmemMatrixD(64, 256) # Distributed: D[x,y,:,:] on CTA x, warpgroup y
209 cg: barrier[2, 2] @ CudaCommitGroup # Distributed: cg[x,y] for CTA x, warpgroup y
210 for cta in cuda_threads(0, 2, unit=cta_in_cluster):
211     for wg in cuda_threads(0, 2, unit=cuda_warpgroup):
212         some_in_order_op_1(B[cta, :, :])
213         example_wgmma(D[cta, wg, :, :], some_A[:, :], B[cta, :, :]) # D += matmul(A, B)
214         Arrive(wgmma_async) >> cg[cta, wg]
215         cs: barrier @ CudaClusterSync
216         Arrive(cuda_in_order) >> cs
217         for cta in cuda_threads(0, 2, unit=cta_in_cluster):
218             for wg in cuda_threads(0, 2, unit=cuda_warpgroup):
219                 Await(cs, cuda_in_order, 0)
220                 some_in_order_op_2(D[cta, wg, :, :])
221                 Await(cs, cuda_in_order, 0)
222                 example_tma_multicast(B[:, :, :], some_gmem[:, :, :]) # Copy some_gmem[:, :] to B[0,:,:] and B[1,:,:]
```

221 The statements connected in blue on the left illustrate safe synchronization in a situation similar
 222 to our first example: the Arrive/Await pair using cs (cluster sync) ensures all accesses to B by
 223 some_in_order_op_1 finish before any thread in the cluster overwrites B using TMA. The state-
 224 ments connected in blue on the right illustrate safe synchronization in a situation similar to our
 225 second example: the Arrive/Await pair using cg (commit group) ensures each warpgroup waits
 226 for its example_wgmma to finish before accessing D[cta, wg...] in some_in_order_op_2.

227 However, the bolded access to **B** by example_wgmma is unsafe. Dotted red arrows illustrate
 228 synchronization that does *not* happen. Because the Arrive on cs uses the timeline cuda_in_order,
 229 the completion of the Arrive does not depend on the prior async wgmma instructions to retire.
 230 Meanwhile, the Await on cg (commit group) occurs too late for it to interact transitively with the
 231 prior cs (cluster sync) Arrive. Therefore, while all *non-async* accesses to B will retire before any
 232 thread proceeds to the TMA multicast, this isn't the case for the async wgmma instructions, whose
 233 B operand could be overwritten unexpectedly by another CTA multicasting to its input memory.
 234 Subtle bugs like this can be difficult to spot in optimized CUDA code.

235 2.3 Optimization Process and Equivalence Checking

236 Exo-GPU programmers can either directly write optimized object code or apply a sequence of sched-
 237 uling transformations to simple initial code. Both approaches grant full control over performance-
 238 critical details. However, the scheduling approach offers significant practical advantages for per-
 239 formance engineering: optimization strategies become reusable functions across similar kernels,
 240 complex transformations decompose into sequences of verified primitives that enable rapid iteration
 241 with correctness guarantees, and the compiler automatically handles complex index calculations
 242 for tiling strategies—especially valuable for GPU optimization. Below, we describe Exo-GPU's
 243 scheduling-based optimization process.

246	$v : \text{Var} ::= x \in \mathbb{X}$	data variable		
247	$y \in \mathbb{Y}$	control variable		
248	$z \in \mathbb{B}$	barrier variable		
249	$r \in \mathbb{W}$	warp variable		
250	$e : \text{DExpr} ::= d$	data value	$c : \text{CExpr} ::= n$	integer
251	$x x[w^*]$	reads	y	reads
252	$e_1 + e_2 e_1 - e_2 e_1 * e_2 e_1 / e_2$	compound expr	$c_1 + c_2 c_1 - c_2 c * n$	affine arith
253	$e_z : \text{ZExpr} ::= z z[w^*]$	reads	$c / n c \bmod n$	quasi affine
254	$e_w : \text{WExpr} ::= r = (n, n, n)$	warp config	$b : \text{BExpr} ::= t$	boolean
255	$n \in \mathbb{Z}$	integer	$b_1 \text{ and } b_2 b_1 \text{ or } b_2$	logical ops
256	$t \in \text{Bool}$	boolean	$c_1 == c_2 c_1 < c_2 c_1 \leq c_2$	relational ops
257	$d \in \mathbb{D}$	data values	$w : \text{WinCoord} ::= c$	point access
			$c_1..c_2$	interval access

Fig. 1. The syntax of variables and expressions of GPU IR. We use * to mean 0 or more.

The scheduling flow in Exo-GPU begins with a simple initial procedure p_1 . The programmer issues a series of *rewrite operations* $R_1 \dots R_{N-1}$ to create transformed procedures $p_2 \dots p_N$.

$$\begin{array}{lll} \text{Rewrites: } & p_1 \xrightarrow{R_1} p_2 \dots \xrightarrow{R_{N-1}} p_N & (\text{Exo-GPU checks}) \quad p_N \\ \text{Behavior: } & \text{seq} [p_1] \equiv \text{seq} [p_2] \dots \equiv \text{seq} [p_N] & \equiv \text{par} [p_N] \end{array}$$

Exo's scheduling rewrite verifies functional equivalence of $\text{seq} [p_1] \dots \text{seq} [p_N]$ under sequential semantics (denoted $\text{seq} [\dots]$). Exo-GPU adds new scheduling operations for parallel and synchronization constructs, but these non-semantics-altering annotations are ignored under $\text{seq} [\dots]$ checks. Then Exo-GPU performs additional verification on the final program p_N . Specifically, synchronization checking ensures $\text{seq} [p_N] \equiv \text{par} [p_N]$, where $\text{par} [\dots]$ denotes parallel semantics. Transitively, this completes the *chain of equivalence* from $\text{seq} [p_1] \equiv \dots \equiv \text{seq} [p_N] \equiv \text{par} [p_N]$, guaranteeing that p_1 's behavior is preserved throughout all transformations.

Equivalence checking relies on three categories of reasoning:

Exo Rewrites: Exo's existing rewrites implement dependency analysis-based equivalence checking, which guards against *dataflow logic bugs*. For example, `reorder_stmts`, which reorders two statements $s_1; s_2$, is only permitted when the effects of the statements commute.

Instruction Substitution: Explicit instruction selection rewrite (replace) lets programmers substitute a code block with an accelerator instruction call. Exo-GPU models instructions via their *behavior* (sequential semantics), per-parameter *memory type* (physical memory and layout), expected collective unit τ_u , and *async* annotations. Exo's unification verifies that the replaced code block's behavior matches the instruction, while Exo-GPU's static analysis ensures appropriate threads execute it (Section 4.1); together preventing *instruction logic errors*.

Exo-GPU Synchronization Check: Since parallel loops and synchronization statements (Fence, `Arrive`, and `Await`) are ignored during sequential checks, synchronization checking must ensure that their usage is valid and does not alter program behavior or introduce race conditions. We verify this via interpretation on the Abstract Machine (Section 5), which protects the program against both *inter- and intra-thread synchronization bugs* for selected concrete problem sizes.

3 GPU IR

GPU IR is the frontend language of Exo-GPU, and examples in Section 2 are written in GPU IR.

3.1 Variables and Expressions

Figure 1 defines the expression syntax of GPU IR. GPU IR explicitly distinguishes between control, data, barrier, and warp expressions and is a static control program. We denote the sets of data, control, barrier, and warp variables by $\mathbb{X}, \mathbb{Y}, \mathbb{B}, \mathbb{W}$, respectively. $x \in \mathbb{X}$ is a data variable, $y \in \mathbb{Y}$

is a control variable, $z \in \mathbb{B}$ is a barrier variable, and $r \in \mathbb{W}$ is a warp variable. The truth values $\text{Bool} \triangleq \{\text{true}, \text{false}\}$. are ranged over by a metavariable t , and n is the metavariable for $\mathbb{Z} \triangleq \{\dots, -1, 0, 1, 2, \dots\}$. The metavariable $d \in \mathbb{D}$ ranges over data values, including 8-, 32-, and 64-bit integers as well as single- and double-precision floating-points.

Control expressions CExpr encompass integer, scalar read, and (quasi-) affine arithmetic operations. Boolean expressions BExpr define basic logical and relational operations on control expressions. Data expressions DExpr are similarly defined, but operations need not be affine. Barrier Expressions ZExpr are only allowed to read, but not composed. Window coordinates w^* (we use $.\ast$ to denote a tuple) used in data and barrier read accesses are specified as a tuple of point-wise or interval control expressions, expressing a windowed access to multi-dimensional arrays. Scalar read is syntactic sugar for an array access of $w^* = \langle \rangle$ (empty tuple).

3.2 Types

All types are fully defined in Appendix A. This section provides a general introduction to the different types in GPU IR. Figure 10 defines data and barrier types. Data types τ_x specify precisions for data variables \mathbb{X} , such as f32 and i32. Barrier types τ_z distinguish a non-explicitly guarded barrier from an explicitly guarded barrier ($\text{barrier}(z)$); the explicitly guarded barrier case is required only for mbarriers. A *collective type* ($\delta \in \Delta$) defines a tuple consisting of a domain and a box, each representing d -dimensional natural numbers $((\mathbb{N}^d, \mathbb{N}^d))$. Together, these define a d -level thread hierarchy within a thread cluster, and a selection of a number of elements on each level. An argument to `cuda_threads` loop τ_u is parameterized by a collective type δ , which is defined in Figure 11. Figures 12–14 classify three categories of memory spaces: π_d for data memories (such as `CudaRmem` for CUDA registers), π_z for barrier completion mechanisms (such as `mbarrier` or `commit_group`), and π_w for special window aliasing (such as `CUtensorMap`). Similar to τ_u , π_d is parameterized by δ .

A qualitative timeline τ_q annotates each *runtime* buffer access. We define distinct τ_q to distinguish between buffer accesses that require different synchronization mechanisms or memory fences to resolve hazards. For example, we distinguish non-async copies from `cp.async` copies (which require `cp.async.wait_all` or similar to wait for), and we distinguish register and SMEM operands of `wmma` instructions (which require `wmma.fence` and `fence.proxy.async`, respectively). Section 5 will formally define how a runtime buffer access instance $x[i_1, \dots, i_n]$ tagged with q_1 states that, at the program point and thread, the access to x occurs under q_1 . Moreover, the sync timelines SyncTL mentioned in Section 2.1, which parameterize synchronization statements, are actually defined as compositions of qualitative timelines (QualTL), as shown in Figure 16.

3.3 Programs

Exo-GPU supports two types of procedures, $p : \text{Proc}$, which models CPU functions (possibly containing CUDA kernel launches), and $g : \text{Instr}$, which models hardware instructions for either CPU or CUDA. Both procedure types share three common components: a statement body that defines sequential behavior, a tuple of control parameters y^* , and a tuple of data parameters x^* . Each data parameter in Proc carries two annotations: τ_x , specifying the required data precision, and π_d , specifying the required memory type for the passed argument.

Instruction parameters (τ_a) also carry both τ_x and π_d annotations, as well as hardware-specific information, namely: out-of-order, convergence, and qualitative timeline information, which all affect only abstract machine semantics for checking (Section 5). The τ_a also contains a distributed collective units tuple (τ_u^*) specifying the CUDA thread hierarchy at which each array dimension is sharded (checked by distributed memory analysis, Section 4.1). The instruction (g) contains annotations for t (a CPU/CUDA flag), a collective unit τ_u specifying the convergent threads required, and π_z and τ_u^* .

344	$s : \text{Stmt} ::= s_1; s_2$	sequencing
345	for y in seq($c_{\text{lo}}, c_{\text{hi}}$) do s	sequential loop
346	for y in cuda_tasks($c_{\text{lo}}, c_{\text{hi}}$) do s	cuda tasks
347	for y in cuda_threads($c_{\text{lo}}, c_{\text{hi}}, \text{unit}=\tau_u$) do s	cuda threads
348	with CudaDeviceFunction(n, e_w^*) do s	CUDA device function block
349	with CudaWarps(n, n, r) do s	Warp Specialization Block
350	if b then s	guard
351	$p(c^*, e^*)$	non-instruction subprocedure call
352	$g(c^*, e^*) \gg e_z$	instruction subprocedure call
353	$x[c^*] = e$	write
354	$x[c^*] += e$	reduce
355	$x = x[c^*] @ \pi_w$	window statement
356	$x : \tau_x[c^*] @ \pi_d$	Data alloc
357	$z : \tau_z[c^*] @ \pi_z$	Barrier alloc
358	free x	Data free
359	free z	Barrier free
360	Fence(τ_z, τ_s)	Non-split barriers
361	Arrive(τ_s, n) $\gg e_z^*$	Arrive
362	Await(e_z, τ_s, n)	Await
363	$\tau_a : \text{Arg} ::= \tau_x$	data type (precision)
364	π_d	data memory type
365	out_of_order $\in \text{Bool}$	out-of-order execution flag
366	convergent $\in \text{Bool}$	implicit thread sync flag
367	τ_u^*	distributed collective units
368	initial_qual_tl $\in \text{QualTL}$	initial qualitative timeline
369	ext_qual_tl $\in \mathcal{P}(\text{QualTL})$	extended qualitative timeline set
370	atomic_qual_tl $\in \mathcal{P}(\text{QualTL})$	atomic qualitative timeline set
371	$p : \text{Proc} ::= \text{proc } y^*, (x : \tau_x @ \pi_d)^* \text{ do } s$	$g : \text{Instr} ::= \text{proc } y^*, (x : \tau_a)^*, t, \tau_u, \pi_z, \tau_u^* \text{ do } s$

Fig. 2. The syntax of GPU IR statements.

3.4 Statements

Figure 2 defines statements $s \in \text{Stmt}$. A statement can sequence ($s_1; s_2$), iterate over loops (seq, cuda_tasks, or cuda_threads), and guard (if b then s). Data effects include indexed writes $x[c^*] = e$, reductions $x[c^*] += e$, and window creation $x = x[c_{\text{lo}} : c_{\text{hi}}] @ \pi_w$. CudaDeviceFunction and CudaWarps control generation and selection of CUDA threads. Synchronization statements Fence, Arrive, and Await get lowered to CUDA synchronization and proxy fence instructions.

CUDA Kernel Structure: All Exo-GPU with `CudaDeviceFunction(...)`:

```
for cta_m in cuda_tasks(...):
    for cta_n in cuda_tasks(...):
        # Device task starts here
        A_smem: f32[128, 32] @ CudaSmemLinear
        # ...
```

code is compiled as CPU code by default. A CudaDeviceFunction block specifies a CPU-side launch of a CUDA kernel. Its body must contain only a single statement: a nest of one or more cuda_tasks loops; cuda_tasks loops must not appear elsewhere. Each iteration of the innermost cuda_tasks loop comprises a device task and is assigned to one CUDA cluster for execution. The *device scope* of a statement is CPU if outside of a CudaDeviceFunction block, and GPU if inside. At CPU scope, all loops must have loop mode seq. The arguments of `CudaDeviceFunction(n, e_w^*)` respectively define the `clusterDim` and, indirectly, the `blockDim` of the CUDA clusters launched. Each warp expression $e_w : r = (n, n, n)$ defines a group of warps named r , with the first n parameter being the number of warps. If nonzero, the latter two n parameters specify that the warps will adjust the register count down or up, respectively, using a `setmaxnreg.dec` or `setmaxnreg.inc` instruction [18]. We infer that `blockDim` is 32 times the total number of warps named.

393 **Thread Control:** Having described the
 394 cuda_tasks loops (inter-cluster parallelism),
 395 we now describe cuda_threads loops and
 396 with CudaWarps (intra-cluster parallelism). A
 397 cuda_threads loop takes its the executing
 398 threads in flight and sub-divides it, assigning
 399 one subdivision to execute each loop iteration
 400 (possibly with left-over, inactivated threads).
 401 The unit parameter adjusts the number of
 402 threads per iteration. The CudaWarps(n, n, r) block restricts its body statement to execute only with
 403 threads residing in the warp variable named by r (which is defined in the CudaDeviceFunction);
 404 the numeric arguments further restrict the warps selected.

405 **Proc & Instruction Calls:** Calls to $p : \text{Proc}$ and $g : \text{Instr}$ are syntactically similar, distinguished
 406 only by the callable's type. Exo-GPU's static analysis enforces that calls to $p : \text{Proc}$ only appear at
 407 CPU scope, while calls to $g : \text{Instr}$ appear at CPU or CUDA scope as appropriate for g . For CUDA
 408 instructions, calls to g must only appear at τ_u -scope, where τ_u is the collective unit specified for g .
 409 Additionally, each data parameter must have the correct precision τ_x and memory type π_d , and the
 410 trailing barrier (if required) must have the correct π_z .

411 **Synchronization Statements:** The user specifies synchronization between threads and/or
 412 between async accelerator instructions by inserting synchronization statements. They take *synchronization timeline* (SyncTL) parameters, defined as compositions of qualitative timelines and a
 413 transitivity (trnstv?) flag (Figure 16). The transitivity flag controls interaction between synchronization statements, detailed in Section 5.

414 Each $\tau_s : \text{SyncTL}$ contains two QualTL sets: the full timeline set (indicated by "full" in (Figure
 415), and a temporal timeline set (indicated by "full" or "temp."). A Fence($\tau_s^{\text{pre}}, \tau_s^{\text{post}}$), or paired
 416 Arrive($\tau_s^{\text{pre}}, _$) and Await($_, \tau_s^{\text{post}}$, $_$) statements, resolves hazards between two accesses to the
 417 same array element when: (1) the first access precedes synchronization and uses a QualTL from
 418 τ_s^{pre} 's full timeline set, and (2) the second access follows synchronization and uses a QualTL from
 419 τ_s^{post} 's full timeline set (for reads) or temporal timeline set (for writes). In hardware terms, the
 420 distinction between the full and temporal timeline sets is due to memory fences. If the prior value of
 421 a buffer element is *overwritten*, without being read, we require only that the overwrite is temporally
 422 ordered after prior accesses to that buffer element, and memory fences may be elided.

423 **Alloc & Free:** An allocation statement begins the lifetime of a new data or barrier variable. For
 424 data allocations, the data memory π_d determines the physical backing memory (registers (RMEM),
 425 shared memory (SMEM), or global memory (GMEM)) and the mapping between multidimensional
 426 tensor coordinates and 1D memory offsets (Figure 12). It also carries an implicit collective type δ ,
 427 specifying which level of the thread hierarchy at which the physical memory type is allocated (e.g.
 428 CTA for shared memory allocations); this is consumed by distributed memory analysis (Section 4.1).
 429 For barrier allocations, the BarrierComp parameter π_z controls the completion mechanism used
 430 for CUDA code translated from Arrive and Await statements (Figure 13). The explicitly-guarded
 431 barrier type is relevant only for certain configurations of mbarrier usage. A free statement ends
 432 the lifetime of a data or barrier variable. Currently, we forbid the user from inserting free statements
 433 manually; these are added automatically in a separate compiler pass.

434 **Window Statement:** A window statement $x_{\text{win}} = x_{\text{data}}[w^*] @ \pi_w$ defines an alias to x_{data} . A
 435 window into x_{win} can be passed as an instruction argument which requires special window type
 436 π_w . Currently, we only use this feature to construct CUTensorMap objects [18] required for TMA
 437 instructions; we parameterize the CUTensorMap type with its swizzle mode and box shape.

```
my_warp_config = [
  CudaWarpConfig("producer", 1, 40, 0),
  CudaWarpConfig("unused", 3, 40, 0),
  CudaWarpConfig("consumer", 8, 0, 232)]
with CudaDeviceFunction(clusterDim=2,
  warp_config=my_warp_config):
```

Fig. 3. Launching clusters of 2 CTAs each, with 1 "producer", 3 "unused", and 8 "consumer" warps per CTA (total blockDim=384). The consumer warps have 232 registers per thread, and the others only 40.

4 COLLECTIVE ANALYSIS

Collective analysis is a static, forward dataflow analysis over a GPU IR procedure. Its results are consumed by (1) a memory analysis, (2) code generation, and (3) an abstract-machine interpreter. The analysis annotates every GPU lexical scope with a collective tiling $\omega \in \Omega$. By default, statements inherit their parent's tiling unchanged; a new tiling is derived only at: device entry (CudaDeviceFunction), thread loops (cuda_threads), and warp-specialization blocks (CudaWarps). The purpose of this analysis is to statically reason about the mapping between work and the threads *within* clusters, so here we ignore cuda_tasks loops, which distribute work across clusters. We uniquely identify a thread within a cluster by its *natural thread index*; a set of such indices comprises a *thread collective* $\mu \in \mathbb{T}$, where $\mathbb{T} \triangleq \mathcal{P}(\mathbb{N})$.

Definition 4.1 (Natural thread index). The *natural thread index* for a CUDA thread is `cluster_ctarank * blockDim.x + threadIdx.x`. (Exo-GPU only parallelizes on the x dimension).

Definition 4.2 (Collective tiling). A *collective tiling* $\omega \in \Omega$ for an M -dimensional domain is an M -tuple of *dimension descriptors*

$$\omega = \langle \mathcal{D}_0, \dots, \mathcal{D}_{M-1} \rangle \quad \text{with} \quad \mathcal{D}_m = (D_m, O_m),$$

where $D_m \in \mathbb{N}$ is the extent of dimension m and $O_m \in \mathcal{O}^*$ is an ordered list of (possibly empty) *dimension operators* $O : \mathbb{Y} \times \mathbb{N}^3$. We write the thread pitch of dimension m as $P_m \triangleq \prod_{i=m+1}^{M-1} D_i$ where $P_{M-1} = 1$.

The dimensions of a collective tiling ω capture how a cluster's threads are partitioned into hierarchical collectives (cluster, block, warp). We support *reshape* to introduce ad-hoc additional hierarchy (e.g. pairs of warps). From there, each dimension's dimension operators summarize the control variables (identified by $y \in \mathbb{Y}$) that iterate on that dimension. The thread pitch of the dimension describes the distance, in units of natural thread indices, between adjacent elements (e.g. a CTA dimension would have thread pitch `blockDim`).

During forward dataflow analysis, new collective tilings are derived for the three special statements mentioned above, while all other statements inherit their parent's tiling. It produces a child collective tiling through the following transformation:

$$\text{derive}_\omega : (\omega^{\text{env}}, \delta^{\text{stmt}}, y, \text{lo}, \text{hi}, \text{tileCount}) \rightarrow \omega'$$

where ω^{env} is the parent scope's collective tiling and δ^{stmt} is the collective type from the statement. The (optional) iterator y and bounds $[\text{lo}, \text{hi}]$ describe a regular slice of linear thread space; $\text{tileCount} \in \mathbb{N}$ is the number of tiles for that slice.

The `cuda_threads` loop and `CudaWarps` block use derive_ω to create a new collective tiling ω based on the one annotating the parent scope. The `CudaDeviceFunction` block derives ω based on launch parameters: ω is 1-D if `clusterDim=1` (domain $D_0=\text{blockDim}$), otherwise 2-D with $(D_0, D_1)=(\text{clusterDim}, \text{blockDim})$; all operator lists start empty.

The implementation of derive_ω proceeds in two steps:

- (1) *Shape alignment*. Make ω^{env} and δ^{stmt} compatible by reshaping via hierarchical splits so that their thread pitches P_m align.
- (2) *Single-dimension refinement*. After alignment, at most one dimension m is newly tiled; the derivation appends exactly one operator to O_m .

Once a tiling ω is derived, it is compiled into a *thread mapping*: $f_\omega : \Sigma \rightarrow \mathbb{T}$, where $\Sigma \triangleq (\mathbb{Y} \rightarrow \mathbb{Z})$ which maps a control environment $\sigma \in \Sigma$ to a runtime thread collective $\mu \in \mathbb{T}$. Equivalently, let $\mathcal{F} \triangleq \{f \mid f : \Sigma \rightarrow \mathbb{T}\}$ and $f_\omega \in \mathcal{F}$. During conversion, each Abstract Machine statement $s^\#$ is annotated with its thread mapping $f_{s^\#} \in \mathcal{F}$. In Section 5.3 we write $f_{s^\#}$ for the thread mapping associated with statement $s^\#$.

491 4.1 Distributed Memory Analysis

492 *Distributed memory analysis* is a static, program-wide consistency check that ensures every use of
 493 CUDA-scoped data and barrier variables is compatible with their memory definitions. Each memory
 494 type π_d specifies a collective type δ_{π_d} . The analysis validates that allocation and use agree on which
 495 threads “own” which memory slices, indexing respects that ownership, and all uses induce the
 496 same mapping from logical indices to CUDA thread identifiers. Analysis runs in four steps:

- 497 (1) **Desugaring instruction call.** To expose the implicit collective requirement encoded by
 498 each hardware instruction to the collective analysis in **step 2**, we rewrite instruction calls
 499 $g(\dots)$ into explicit loops. Each arguments to the instruction call are wrapped around with
 500 `cuda_threads`, with their collective units specified by $g.r_u^*$ in the instruction specification.
- 501 (2) **Collective analysis.** Run collective analysis and annotate each scope with $\omega \in \Omega$.
- 502 (3) **Triple collection.** For each data or barrier variable, record the *access triple* of all of use
 503 sites. We use \mathcal{T}_v to denote a set of those triples for a variable v ; these sets for all the data and
 504 barrier variables are the sole inputs to **step 4**. Each triple (n^*, ω, c^*) denotes: the subdivided
 505 dimensions n^* , the use-site tiling ω , and observed index coordinates c^* . For each use site:
 - 506 • **Data.** Compute n^* from the memory’s collective type δ_{π_d} and the use-site tiling ω .
 - 507 • **Barriers.** Treat all dimensions as subdivided (every axis participates in distribution).
- 508 (4) **Triple analysis.** For each CUDA-scoped data variable v , we require: (i) consistency of the
 509 allocation w.r.t. the memory’s δ_{π_d} , (ii) consistency of data or barrier accesses across sites
 510 (by checking all triples in \mathcal{T}_v), and (iii) all triples in \mathcal{T}_v must derive one and only one thread
 511 pitch tuple that summarizes how incrementing logical indices advances natural thread IDs.

512 As a result, distributed memory analysis rejects programs that (i) mismatch allocation and accesses
 513 with their memory declaration, (ii) inconsistently index the same data or barrier across sites, or
 514 (iii) rely on missing/extra CUDA-thread iterators. Passing guarantees that the program’s memory
 515 behavior is coherent with its collective structure and declared memory types.

517 4.2 Code Generation to CUDA Code

518 **Lowering `cuda_threads` Loops:** The corre- `if (int y = f(blockIdx, threadIdx); g(y)) {`
 519 spondence between parallel loops and threads `lower(s); }`

520 has thus far been expressed in terms of thread mappings of type $\Sigma \rightarrow \mathbb{T}$, which infer a set of
 521 active threads from the control environment σ . However, the generated CUDA C++ implements the
 522 inverse of this mapping, inferring the value of a control variable y from the thread index instead.
 523 Each Exo-GPU loop of the form `for y in cuda_threads(lo, hi, unit=t_u) do s` lowers to
 524 CUDA C++ as shown in the inset right. Here, f is a function of CUDA’s built-in `blockIdx` and
 525 `threadIdx` variables, and g is a boolean condition on y that disables threads not assigned to execute
 526 any iteration of the body. Where possible, f is 0 and g is 1, to facilitate uniform branching.

527 **Warp Specialization:** When a device function uses multiple warp variables $r_1, \dots, r_W \in \mathbb{W}$, we
 528 generate W -many CUDA C++ code paths from a single Exo-GPU device function, each specialized
 529 for (and executed by) the threads assigned to one warp variable. Each path uses PTX’s `setmaxnreg`
 530 instruction to vary per-thread register counts, and omits all code paths guarded by a `with CudaWarp`
 531 block holding code not intended for the current warp. This allows the PTX assembler to statically
 532 verify that register-heavy instructions (e.g. `wgmma`) don’t appear on low-register code paths.

533 **Persistent Kernels and `cuda_tasks` Loops:** The generated CUDA C++ device functions imple-
 534 ment a persistent kernel design that launches exactly the number of thread block clusters needed
 535 to saturate the device. Following the approach of CUTLASS grouped kernel schedulers [16], we
 536 implement a C++ task generator object that generates a series of device task coordinates for thread
 537 block clusters to execute. The current implementation orders tasks lexicographically and assigns
 538 them round-robin to thread block clusters for execution. While we leave it as future work to

540	$\tau_v : VL ::=$	fully_ordered temporally_ordered unordered atomic_only invisible	visibility levels
541	$e^\# : Expr^\# ::= e_d^\# \mid e_z^\#$	where $e_d^\# \triangleq x[w^*]$ $e_z^\# \triangleq z[w^*]$	barrier and data accesses
542	$s^\# : Stmt^\# ::= s_1^\# ; s_2^\#$		sequencing
543	for y in loop(c_{lo}, c_{hi}) do $s^\#$		loop
544	if b then $s^\#$		guard
545	IncTaskID		increment the task ID
546	Alloc($e^\#$)		Updates SyncEnv for Alloc
547	RecordRead($\tau_v, t, e^\#, \tau_q, \tau_q^*, e_z^\#$)		Updates SyncEnv with Read
548	RecordMutate($\tau_v, t, e^\#, \tau_q, \tau_q^*, e_z^\#$)		Updates SyncEnv with Mutate
549	ClearReads($e^\#$)		Remove state added by RecordRead
550	ClearMutates($e^\#$)		Remove state added by RecordMutate
551	Fence($t, \tau_q^*, \tau_q^*, \tau_q^*$)		Non-split barriers
552	Arrive($t, \tau_q^*, e_z^\#$)		Arrive
553	Await($e_z^\#, \tau_q^*, \tau_q^*, n$)		Await
554	CheckReads($\tau_v, t, e^\#, \tau_q^*$)		Checks visibility of Reads in SyncEnv
555	CheckMutates($\tau_v, t, e^\#, \tau_q^*$)		Checks visibility of Mutates in SyncEnv
556	CheckBarrier($e_z^\#$)		Checks the consistency of arrive and await
557	$p^\# : Proc^\# ::= proc y^*$		arguments are control-only
558	do $s^\#$		

559 Fig. 4. Syntax of Abstract Machine IR (AMIR). Variables, types, and expressions (c, b, w) use the same definition
560 as GPU IR. Visibility levels are denoted by the type $\tau_v \in VL$ and range over the five constructors listed above.

561 provide a mechanism for programmers to customize this ordering, such customization would be
562 unconstrained by frontend’s quasi-affine indexing restrictions since cuda_tasks loops impose no
563 semantic ordering, thereby enabling techniques like Morton swizzling.

564 **Shared Memory Allocations:** Device functions generated by Exo-GPU use only dynamic shared
565 memory for SMEM allocation. The Exo-GPU compiler deduces the required SMEM allocation size
566 and statically assigns offsets into this allocation for each SMEM-backed variable. Variables with
567 non-overlapping lifetimes may share the same memory locations; to ensure safe aliasing, we
568 prohibit any thread in the cluster from passing an SMEM free statement until all reads and writes
569 to the freed variable have retired, as enforced by the Abstract Machine (Section 5). This is necessary
570 because freed SMEM may be immediately reused by any thread in the cluster. We note that the
571 compiler’s aliasing may be suboptimal, and the cluster-wide safety requirement may be overly
572 conservative (e.g., for CTA-local variables). Providing programmers explicit control over SMEM
573 lifetime and aliasing is left as future work.

5 ABSTRACT MACHINE

575 To guarantee sequential-parallel equivalence, Exo-GPU performs synchronization checking via
576 Abstract Machine interpretation. This section introduces the AMIR grammar (Section 5.1), the trans-
577 lation from GPU IR (Section 5.2), and the AMIR execution semantics (Section 5.3). We translate GPU
578 IR into AMIR solely for validation: the frontend language remains simple, while synchronization
579 reasoning is factored into explicit AMIR operations that are orthogonal to value computation.

5.1 Abstract Machine Grammar

583 Figure 4 defines AMIR grammar. It follows GPU IR for control c , booleans b , window coordi-
584 nates w , and all variable/type definitions (Figures 1, 2). AMIR defines only windowed access
585 expressions, written $e_d^\# \triangleq x[w^*]$ (data access) and $e_z^\# \triangleq z[w^*]$ (barrier access). AMIR introduces
586 visibility levels $\tau_v \in VL$, which are totally ordered: $\text{invisible} < \text{atomic_only} < \text{unordered} <$
587 $\text{temporally_ordered} < \text{fully_ordered}$.

GPU IR	Abstract Machine IR
589 $s_1; s_2$	$T_s(s_1); T_s(s_2)$
590 $\text{for } y \text{ in seq}(c_{\text{lo}}, c_{\text{hi}}) \text{ do } s$	$\text{for } y \text{ in loop}(c_{\text{lo}}, c_{\text{hi}}) \text{ do } T_s(s)$
591 $\text{for } y \text{ in cuda_tasks}(c_{\text{lo}}, c_{\text{hi}}) \text{ do } s$	$\text{for } y \text{ in loop}(c_{\text{lo}}, c_{\text{hi}}) \text{ do } (\text{IncTaskID}; T_s(s))$
592 $\text{for } y \text{ in cuda_threads}(c_{\text{lo}}, c_{\text{hi}}, \tau_u) \text{ do } s$	$\text{for } y \text{ in loop}(c_{\text{lo}}, c_{\text{hi}}) \text{ do } T_s(s)$
593 $x[c^*] \diamond e \text{ where } \diamond \in \{=, +\}$	$\begin{aligned} &;_{e_1^{\#} \in T_{\text{ex}}(e)} (\text{CheckMutates}(\tau_v^{\text{pre}}, \text{false}, e_1^{\#}, \{T_{\text{qin}}(e_1^{\#})\})) \\ &\quad \text{RecordRead}(\tau_v^{\text{post}}, \text{false}, e_1^{\#}, T_{\text{qin}}(e_1^{\#}), \emptyset, \emptyset) \\ &;_{e_2^{\#} \in T_{\text{ex}}(x[c^*])} (\text{CheckReads}(\tau_v^{\text{pre}}, \text{false}, e_2^{\#}, \{T_{\text{qin}}(e_2^{\#})\})) \\ &\quad \text{CheckMutates}(\tau_v^{\text{pre}}, \text{false}, e_2^{\#}, \{T_{\text{qin}}(e_2^{\#})\}) \\ &\quad \text{ClearReads}(e_2^{\#}); \\ &\quad \text{ClearMutates}(e_2^{\#}); \\ &\quad \text{RecordMutate}(\tau_v^{\text{post}}, \text{false}, e_2^{\#}, T_{\text{qin}}(e_2^{\#}), \emptyset, \emptyset); \end{aligned}$
594 $, \text{ where } \tau_v^{\text{post}} = \text{fully-ordered and}$	$\tau_v^{\text{pre}} = \text{fully-ordered if } +=, \text{ else temporally-ordered}$
595 602	603
604 $\text{if } b \text{ then } s$	$\text{if } b \text{ then } T_s(s)$
605 $\text{with CudaDeviceFunction}(n, e_w^*) \text{ do } s$	$\text{Fence}(\text{true}, \text{Qcs} \cup \{\text{cpu_in_order_qual}\}, \text{Qcs}, \text{Tcs});$
606 $T_s(s);$	$\text{Fence}(\text{true}, \text{Qcs}, \text{Qcs}, \text{Tcs});$
607 $\text{, where Qcs} \triangleq \text{T}_{\text{qfull}}(\text{cuda_stream_sync}), \text{Tcs} \triangleq \text{T}_{\text{qtmp}}(\text{cuda_stream_sync})$	$\text{, where Qcs} \triangleq \text{T}_{\text{qfull}}(\text{cuda_stream_sync}), \text{Tcs} \triangleq \text{T}_{\text{qtmp}}(\text{cuda_stream_sync})$
608 $\text{with CudaWarp}(n, n, r) \text{ do } s$	$\text{if true then } T_s(s)$
609 611	612
610 $g(c^*, e^*) \gg e_z$	$\begin{aligned} &;_{e^{\#} \in T_{\text{ex}}(e_z)} \text{RecordRead}(\text{fully-ordered}, \text{false}, e^{\#}, \emptyset, \emptyset, T_e(e_z)) \\ &;_{i=0}^{\cdot \text{len}(e^*)} T_{\text{arg}}(g.p_i, e_i, e_z) \end{aligned}$
611 613	614
612 $x : \tau_x[c^*] @ \pi_d$	$\text{Alloc}(x[c^*])$
613 $z : \tau_z[c^*] @ \pi_z$	$\text{Alloc}(z[c^*])$
614 616	617
615 $\text{free } x$	$\begin{aligned} &;_{e^{\#} \in T_{\text{smem}}(x[:*])} (\text{CheckReads}(\tau_v^{\text{free}}, \text{false}, e^{\#}, \{T_{\text{qin}}(e^{\#})\})) \\ &\quad \text{CheckMutates}(\tau_v^{\text{free}}, \text{false}, e^{\#}, \{T_{\text{qin}}(e^{\#})\}); \end{aligned}$
616 618	619
617 $\text{free } z$	$\begin{aligned} &\text{CheckBarriers}(T_e(z[:*])); \\ &;_{e^{\#} \in T_{\text{smem}}(z[:*])} (\text{CheckReads}(\tau_v^{\text{free}}, \text{false}, e^{\#}, \{T_{\text{qin}}(e^{\#})\})) \\ &\quad \text{CheckMutates}(\tau_v^{\text{free}}, \text{false}, e^{\#}, \{T_{\text{qin}}(e^{\#})\}); \end{aligned}$
618 621	622
619 $\text{Fence}(\tau_s^{\text{pre}}, \tau_s^{\text{post}})$	$\text{Fence}(T_{\text{tr}}(\tau_s^{\text{pre}}), \text{T}_{\text{qfull}}(\tau_s^{\text{pre}}), \text{T}_{\text{qfull}}(\tau_s^{\text{post}}), \text{T}_{\text{qtmp}}(\tau_s^{\text{post}}))$
620 623	624
621 $\text{Arrive}(\tau_s, n) \gg e_z^*$	$\begin{aligned} &;_{e^{\#} \in T_{\text{ex}}(e_z^*)} \text{RecordRead}(\text{fully-ordered}, \text{false}, e^{\#}, \text{T}_{\text{qarr}}(\tau_s), \emptyset, \emptyset) \\ &\quad \text{Arrive}(T_{\text{tr}}(\tau_s), \text{T}_{\text{qfull}}(\tau_s), T_e(e_z^*)); \end{aligned}$
622 625	626
623 $\text{Await}(e_z, \tau_s, n)$	$\begin{aligned} &;_{e^{\#} \in T_{\text{ex}}(e_z)} \text{RecordRead}(\text{fully-ordered}, \text{false}, e^{\#}, T_{\text{qin}}(e^{\#}), \emptyset, \emptyset) \\ &\quad \text{Await}(T_e(e_z), \text{T}_{\text{qfull}}(\tau_s), \text{T}_{\text{qtmp}}(\tau_s), n); \end{aligned}$
624 627	628
625 629	<p>Fig. 5. $T_s : \text{Stmt} \rightarrow \text{Stmt}^{\#}$ (statement conversion). All <i>conversion</i> functions use the T_{-} prefix (Figures 18–20). $\tau_v^{\text{free}} = \text{temporally-ordered}$</p>
626 630	
627 631	<p>AMIR has no hardware-instruction procedures (g in GPU IR) and no subprocedure calls. Procedures $p^{\#}$ take control-only arguments. The statement (Figure 4) consists of: (i) structural statements—sequencing, loop, and guard (ii) recording statements that update the synchronization environment SyncEnv-Alloc, RecordRead, RecordMutate, Fence, Arrive, and Await; and (iii) checking statements that query SyncEnv and fail if the required visibility obligations are not met; otherwise they are no-ops: CheckBarrier, CheckReads, and CheckMutates.</p>
628 632	
629 633	
630 634	
631 635	
632 636	
633 637	

638 5.2 Conversion from GPU IR to Abstract Machine IR

639 We describe how GPU IR expressions (Section 5.2.1), statements (Section 5.2.2), and instruction
 640 arguments (Section 5.2.3) are converted. Before conversion, we apply two trivial preprocessing
 641 steps to GPU IR: (i) Inline all window statements, and (ii) Inline all subprocedure calls that occur
 642 outside any CudaDeviceFunction block. Throughout this section (and in figures) we use the
 643 following notation. For a finite, ordered variables $R = \langle r_0, \dots, r_{k-1} \rangle$ and a statement template
 644 $S(\cdot), ;_{i=0}^k S(x) \triangleq S(r_0) ; S(r_1) ; \dots ; S(r_{k-1})$. If $R = \emptyset$, the result is no-op. The intent is
 645 purely left-to-right sequential composition at AMIR conversion time. When unambiguous, we write
 646 $f(A) = \{f(a) \mid a \in A\}$ for the pointwise image of a set.
 647

648 5.2.1 *Expression Conversion.* Figure 17 defines $T_e : \text{DExpr} \cup \text{ZExpr} \rightarrow \mathcal{P}(\text{Expr}^\#)$, which extracts
 649 the windowed AMIR accesses $e^\# \in \{x[w^*], z[w^*]\}$: scalars d contribute nothing (\emptyset); a bare name x
 650 or z yields the degenerate accesses $x[\langle \rangle]$ or $z[\langle \rangle]$; explicit indexings $x[w^*]$ and $z[w^*]$ are preserved;
 651 and for arithmetic $e_1 \text{ op } e_2$ the sets union, $T_e(e_1) \cup T_e(e_2)$. T_e is set-valued (order and duplicates are
 652 irrelevant), leaves the value expression unchanged, and merely supplies the converted $\text{Expr}^\#$ used
 653 by RecordRead/RecordMutate and subsequent visibility checks.

654 5.2.2 *Statement Conversion.* Figure 5 gives a structural translation $T_s : \text{Stmt} \rightarrow \text{Stmt}^\#$ from GPU
 655 IR to AMIR. Helper functions referenced by Figure 5 are defined in Figure 18. Sequencing and
 656 conditionals are preserved, while all loops are normalized to the abstract loop form. Warp/block
 657 scopes are dropped and replaced with a guard whose condition is `true`. Assignments $x[c^*] \diamond e$
 658 ($\diamond \in \{=, +=\}$) are lowered to explicit read/write effects. We expand source and destination with T_e
 659 and remove sync-exempt expressions via T_{ex} . *Sync-exempt memories* are those whose accesses can
 660 be assumed safe without checking: CudaGridConstant, CudaClusterSync, and CudaCommitGroup.
 661 *Shared memories* are the following: CudaBasicSmem, CudaSmemAtomicity16B, CudaSmemLinear,
 662 Sm90_SmemSwizzled(B), or CudaMbarrier.

663 Hardware instruction calls ignore control arguments and pair the instruction's parameter definition
 664 and the arguments via T_{arg} . The entry and exit of CudaDeviceFunction is bracketed with fences
 665 with `cuda_stream_sync`, capturing both the CPU-to-GPU fence implied by the kernel launch, and
 666 the serialization of the CUDA kernel with respect to prior and subsequent CUDA kernels and
 667 API calls (Note that Exo-GPU currently uses only one CUDA stream). During the conversion, we
 668 record the scope of each statement using a global environment $\text{Scope} : \text{Stmt}^\# \rightarrow \{\text{CPU}, \text{CUDA}\}$.
 669 Statements outside the CudaDeviceFunction block are CPU-scoped, while those inside are GPU-
 670 scoped. The scope mapping is used in Definition 5.2. Fence, Arrive, and Await translate a sync
 671 timeline (τ_s) into a qualitative timeline set (τ_q^*) . T_{tr} queries whether a sync timeline is transitive;
 672 T_{qfull} and T_{qtmp} materialize the full and temporal QualTL sets, respectively. Arrive selects its arrival
 673 qualitative timeline via T_{qarr} to sync-check the barrier itself, thereby preventing use-after-free bugs.
 674

675 5.2.3 *Instruction Argument Conversion.* Figure 19 expands the conversion $T_{\text{arg}}(g.p_i, e_i, e_z)$ from a
 676 GPU IR instruction call argument to the AMIR statements. The auxiliary projections and predicates
 677 referenced in the figure— T_{ext} , T_{atom} , T_{init} , T_{ooo} , and T_{cvg} —are defined in Figure 20. For each non-sync
 678 exempt expression $e^\# \in T_{\text{ex}}(e_i)$, the conversion emits a sequence of checks and effect-recording
 679 operations which depends on two properties of the parameter $g.p_i$: its *access mode* (read-only vs.
 680 write-only/read-write) and whether it is *atomic*. The access mode of $g.p_i$ is determined by a simple
 681 intraprocedural static analysis over instruction body (behavior) $g.s$: if $g.p_i$ is only read (and never
 682 written or reduced), it is classified as read-only; if it is written but never read or reduced, it is
 683 write-only; otherwise it is read-write. The atomic case is selected exactly when $T_{\text{atom}}(g.p_i) \neq \emptyset$.

684 5.2.4 *Program Conversion.* The GPU IR's program $\text{proc } y^*, (x : \tau_x)^* ; \text{do } s$ is translated into an
 685 AMIR program $\text{proc } y^* ; \text{do } s^\#$ where only control arguments are retained. Non-control arguments
 686

$$\begin{array}{c}
687 \quad \frac{}{\langle n, \sigma \rangle \Downarrow_{\mathbb{Z}} n} \text{C-INT} \quad \frac{\sigma(y) = n}{\langle y, \sigma \rangle \Downarrow_{\mathbb{Z}} n} \text{C-READ} \quad \frac{\langle c_1, \sigma \rangle \Downarrow_{\mathbb{Z}} n_1 \quad \langle c_2, \sigma \rangle \Downarrow_{\mathbb{Z}} n_2 \quad \text{op} \in \{+, -, *, /\}}{\langle c_1 \text{ op } c_2, \sigma \rangle \Downarrow_{\mathbb{Z}} (n_1 \text{ op } n_2)} \text{C-AFF} \\
688 \\
689 \\
690 \quad \frac{}{\langle t, \sigma \rangle \Downarrow_{\text{Bool}} t} \text{B-CONST} \quad \frac{\langle b_1, \sigma \rangle \Downarrow_{\text{Bool}} t_1 \quad \langle b_2, \sigma \rangle \Downarrow_{\text{Bool}} t_2 \quad \text{op} \in \{\text{and}, \text{or}\}}{\langle b_1 \text{ op } b_2, \sigma \rangle \Downarrow_{\text{Bool}} \overline{\text{op}}(t_1, t_2)} \text{B-LOG} \\
691 \\
692 \\
693 \quad \frac{\langle c_1, \sigma \rangle \Downarrow_{\mathbb{Z}} n_1 \quad \langle c_2, \sigma \rangle \Downarrow_{\mathbb{Z}} n_2 \quad \text{op} \in \{=, <, \leq\}}{\langle c_1 \text{ op } c_2, \sigma \rangle \Downarrow_{\text{Bool}} (n_1 \text{ op } n_2)} \text{B-REL} \quad \frac{\langle c, \sigma \rangle \Downarrow_{\mathbb{Z}} i}{\langle c, \sigma \rangle \Downarrow_I \{i\}} \text{W-POINT} \\
694 \\
695 \\
696 \quad \frac{\langle c_1, \sigma \rangle \Downarrow_{\mathbb{Z}} i_1 \quad \langle c_2, \sigma \rangle \Downarrow_{\mathbb{Z}} i_2}{\langle c_1..c_2, \sigma \rangle \Downarrow_I \{i \in \mathbb{Z} \mid i_1 \leq i \leq i_2\}} \text{W-RANGE} \quad \frac{\forall j \in \{1..n\}. \langle w_j, \sigma \rangle \Downarrow_I W_j}{\langle w_1, \dots, w_n, \sigma \rangle \Downarrow_{I^n} W_1 \times \dots \times W_n} \text{W-TUPLE} \\
697 \\
698 \\
699 \quad \frac{a \in \mathbb{X} \cup \mathbb{B} \quad \langle w_1, \dots, w_n, \sigma \rangle \Downarrow_{I^n} \mathbf{W}}{\langle a[w_1, \dots, w_n], \sigma \rangle \Downarrow_{\text{Acc}} \{a \mapsto \vec{i} \mid \vec{i} \in \mathbf{W}\}} \text{E#-Acc} \\
700 \\
701 \\
702 \quad \text{Fig. 6. The big-step operational semantics for expressions.} \\
703
\end{array}$$

$(x : \tau_x)^*$ are ignored during the conversion. Control variables are preserved, since GPU IR and AMIR share the same control variables set \mathbb{Y} . T_s is applied to the program body to convert s to s^* .

5.3 Abstract Machine Semantics

Definition 5.1 (Control–Value Environment). Let \mathbb{Z} be the set of control value and \mathbb{Y} the set of control variables. $\sigma \in \Sigma \triangleq \mathbb{Y} \rightarrow \mathbb{Z}$.

Definition 5.2 (Global Threads Collective). Let \mathbb{I} be the set of task IDs and \mathbb{T} the set of all (local) thread IDs (thread collective). The set of global thread IDs is $\mathbb{G} \triangleq \mathbb{I} \times \mathbb{T}$. For each statement s^* , thread mapping $f_{s^*} : \Sigma \rightarrow \mathbb{T}$ returns the set of local threads that execute s^* under σ (f_{s^*} defined in Section 4). The scope mapping scope : Stmt $^* \rightarrow \{\text{CPU}, \text{GPU}\}$ is initialized during the statement conversion to indicate whether each statement belongs to the CPU or GPU scope. Given σ and $i \in \mathbb{I}$, define the corresponding global threads

$$g_{s^*}(\sigma, i) \triangleq \begin{cases} \{(i, t) \mid t \in f_{s^*}(\sigma)\} & \text{if scope}(s) = \text{GPU} \\ \mathbb{G} & \text{otherwise} \end{cases}$$

Definition 5.3 (Synchronization Environment). Let \mathbb{B} be the set of barrier names and \mathbb{X} the set of data variables. Define

$$\mathbb{P} : \mathbb{B} \rightarrow \mathbb{Z}^n \rightarrow \mathcal{P}(\mathbb{N}) \quad \text{and} \quad \mathbb{S} : \mathbb{G} \rightarrow \text{QualTL} \rightarrow \text{VL},$$

where $\mathbb{P}(b, c^*)$ is the set of observed arrive counts at barrier access $b[c^*]$, and $\mathbb{S}(g, \tau_q)$ is the visibility level for the thread with global ID $g \in \mathbb{G}$ on a qualitative timeline τ_q (Figure 4). Let

$$\mathbb{R} \triangleq \text{QualTL} \times \mathbb{S} \times \mathbb{P}$$

be the set of *visibility records*, written (q, f, p) . The synchronization environment is the map

$$\rho : (\mathbb{X} \cup \mathbb{B}) \rightarrow \mathbb{Z}^n \rightarrow \mathcal{P}(\mathbb{R}) \times \mathcal{P}(\mathbb{R}) \times \mathbb{N}^2,$$

sending a name and index to a tuple of (read visibility record (r): \mathbb{R} , mutate visibility record (m): \mathbb{R} , barrier count (b): n^2).

The semantics follows a standard big-step style where judgments take the form $\langle e^*, \sigma \rangle \Downarrow v$ for expressions and $\langle s^*, i, \sigma, \rho \rangle \Downarrow i', \sigma', \rho'$ for statements, indicating that expression e^* evaluates to value v in state σ , and statement s^* transforms state σ to σ' , ρ to ρ' , and i to i' , respectively.

736		
737	$\exists (_, f, _) \in \rho(W_{e^*}).r ((t = \text{false} \wedge \exists g \in g_{s^*}(\sigma, \iota), \forall \tau_q \in \tau_q^* \mid f(g, \tau_q) \not\leq \tau_v)$	
738	$\langle e^#, \sigma \rangle \Downarrow_{\text{Acc}} W_{e^*}$	$\vee (t = \text{true} \wedge \forall g \in g_{s^*}(\sigma, \iota), \forall \tau_q \in \tau_q^* \mid f(g, \tau_q) \not\leq \tau_v)) \Downarrow_{\text{Bool}} \text{true}$
739		CHECKREADS
740		$\langle \text{CheckReads}(\tau_v, t, e^#, \tau_q^*), \iota, \sigma, \rho \rangle \Downarrow \text{error}$
741	$\exists (_, f, _) \in \rho(W_{e^*}).m ((t = \text{false} \wedge \exists g \in g_{s^*}(\sigma, \iota), \forall \tau_q \in \tau_q^* \mid f(g, \tau_q) \not\leq \tau_v)$	
742	$\langle e^#, \sigma \rangle \Downarrow_{\text{Acc}} W_{e^*}$	$\vee (t = \text{true} \wedge \forall g \in g_{s^*}(\sigma, \iota), \forall \tau_q \in \tau_q^* \mid f(g, \tau_q) \not\leq \tau_v)) \Downarrow_{\text{Bool}} \text{true}$
743		CHECKMUTATES
744		$\langle \text{CheckMutates}(\tau_v, t, e^#, \tau_q^*), \iota, \sigma, \rho \rangle \Downarrow \text{error}$
745	$\langle e_z^#, \sigma \rangle \Downarrow_{\text{Acc}} W_{e_z^#}$	$(\exists (a, w) \in \rho(W_{e_z^*}).b \mid a \neq w) \Downarrow_{\text{Bool}} \text{true}$
746		CHECKBARRIER
747		$\langle \text{CheckBarrier}(e_z^#), \iota, \sigma, \rho \rangle \Downarrow \text{error}$

Fig. 7. Big-step rules for access visibility and barrier consistency. Successful checks leave (ι, σ, ρ) unchanged; any violation reduces the configuration to error state.

5.3.1 *Expression semantics.* Figure 6 gives big-step judgements $\langle e, \sigma \rangle \Downarrow_{\tau} v$. Integer and boolean literals evaluate to themselves (C-INT, B-CONST); variables read from the store (C-READ). Arithmetic evaluates both operands to integers and then applies $\text{op} \in \{+, -, *, /\}$ (C-AFF). Boolean connectives apply the usual truth functions for and/or (B-LOG), and comparisons $\text{op} \in \{==, <, \leq\}$ compare integer results to yield booleans (B-REL). Windows denote index sets \mathcal{I} : a point yields $\{i\}$ (W-POINT); a range $c_1..c_2$ yields the inclusive set $\{i \in \mathbb{Z} \mid i_1 \leq i \leq i_2\}$ (W-RANGE); and an n -tuple of windows denotes the Cartesian product $W_1 \times \dots \times W_n$ (W-TUPLE). The only nonstandard part is E#-Acc: given $a \in \mathbb{X} \cup \mathbb{B}$ and a window tuple \mathbf{W} , it *unpacks* the window into the set of concrete accesses $\{\{a \mapsto \vec{i} \mid \vec{i} \in \mathbf{W}\} \mid \vec{i} \in \mathbf{W}\}$ of type $\mathbb{X} \cup \mathbb{B} \rightarrow \mathbb{Z}^*$.

5.3.2 *Statement semantics.* Figure 21 gives big-step operational semantics for a loop, sequencing, an explicit task-ID increment, and a guard. For $\text{for } y \text{ in loop}(c_{\text{lo}}, c_{\text{hi}}) \text{ do } s^*$, the bounds evaluate in σ to integers m and n ; the loop ranges over the *half-open* interval $[m, n]$: when $m < n$ (LOOPSTEP) the body executes once with $y \mapsto m$, producing (ι', σ', ρ') , and the loop recurs on $(m+1) \dots n$; when $m \geq n$ (LOPDONE) it terminates with no effect. Sequencing (SEQ) threads the triple (ι, σ, ρ) from the first statement into the second. The guard (IF-TRUE/IF-FALSE) evaluates b in σ and either executes s^* or behaves as no-op. The only non-standard rule, INCTASKID, increments the task identifier ($\iota' = \iota + 1$) while leaving σ and ρ unchanged.

Figure 22 shows the rest of statement semantics. Alloc evaluates each extent c_i to an integer n_i (under $\Downarrow_{\mathbb{Z}}$), forms the index set $I = \{(v_1, \dots, v_k) \mid 0 \leq v_i < n_i\}$, and initializes the per-access visibility record for x by updating ρ so that, for every $\mathbf{n} \in I$, $\rho(x, \mathbf{n}) = (\emptyset, \emptyset, (0, 0))$; the thread id ι and store σ are unchanged. ClearReads first resolves the accessed locations via $\langle e^#, \sigma \rangle \Downarrow_{\text{Acc}} W_{e^*}$ and, for each $(x, \mathbf{n}) \in W_{e^*}$, replaces $\rho(x, \mathbf{n}) = (r, m, b) \in \mathbb{R}$ with (\emptyset, m, b) . ClearMutates is analogous but replaces it with (r, \emptyset, b) . RECORDREAD and RECORDMUTATE first evaluate the accessor e^* and e_z^* to access sets W_{e^*} and $W_{e_z^*}$ (via \Downarrow_{Acc}). They then update the visibility map ρ at each key $(x, \mathbf{n}) \in W_{e^*}$ using the new record constructor \mathcal{R} defined in Appendix B.

Fence, Arrive, and Await update ρ solely via $\text{lift}(\rho, \lambda)$ (defined in Appendix B), which applies λ pointwise to both the read and mutate visibility sets. In the following, \mathcal{W} decides when augmentation is permitted, \mathcal{A} raises visibility to *fully_ordered* or *temporally_ordered*. For $\text{Fence}(t, \tau_q^{\text{pre}*}, \tau_q^{\text{full}*}, \tau_q^{\text{temp}*})$, $\lambda(r) = \mathcal{A}(r, g^{\text{exec}*}, \tau_q^{\text{full}*}, \tau_q^{\text{temp}*})$ iff the witness $\mathcal{W}(t, g^{\text{exec}*}, \tau_q^{\text{pre}*}, r)$ holds, otherwise $\lambda(r) = r$; thus visibility is raised by joining $f \vee f_{\text{aug}}$. $\text{Arrive}(t, \tau_q^{\text{pre}*}, e_z^{**})$ and $\text{Await}(e_z^*, \tau_q^{\text{full}*}, \tau_q^{\text{temp}*}, n)$ are defined similarly in Appendix B, updating the access visibility appropriately.

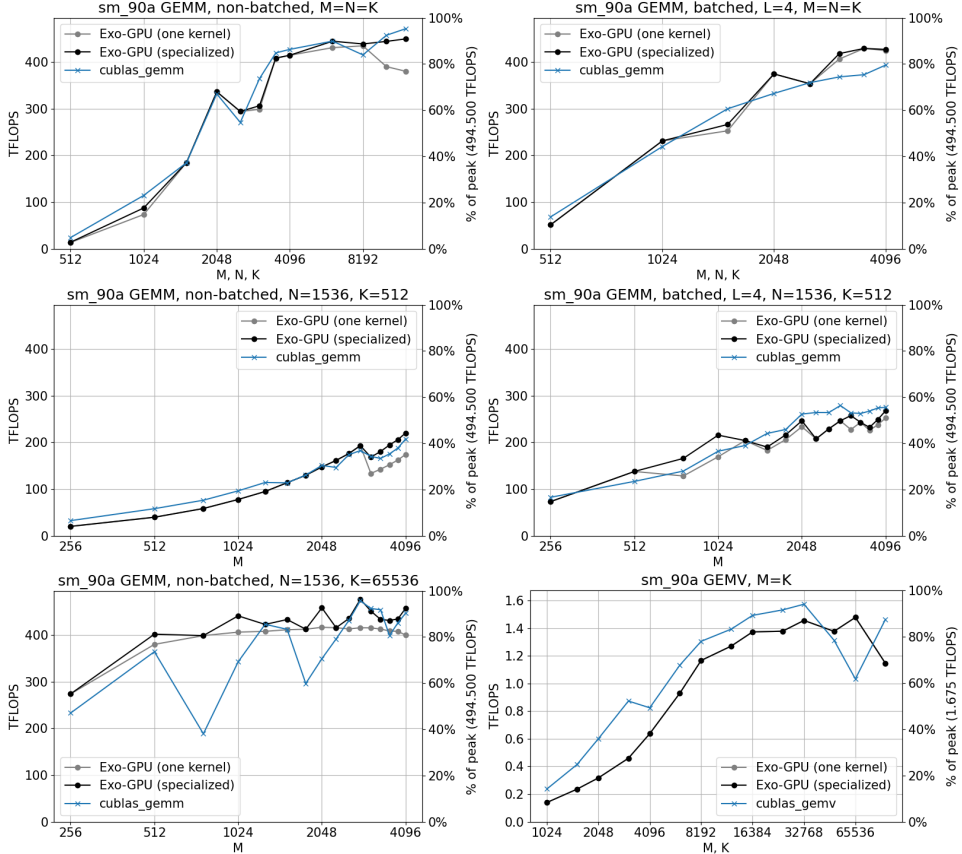


Fig. 8. Performance by varying problem size on a sm_90a GPU.

5.3.3 *Checks.* Figure 7 gives three pure checks that either signal error or leave (ι, σ, ρ) unchanged. CHECKREADS evaluates $e^\#$ to access $W_{e^\#}$ and raises error when some $(_, f, _) \in \rho(W_{e^\#}).r$ fails to supply visibility at least τ_v for all timelines $\tau_q \in \tau_q^*$. CHECKMUTATES is analogous but ranges over mutate visibility record $\rho(W_{e^\#}).m$. CHECKBARRIER evaluates $e_z^\#$ and signals error iff some $(a, w) \in \rho(W_{e_z^\#}).b$ has $a \neq w$, i.e., the recorded *arrive* and *await* counts disagree.

5.3.4 *Program semantics.* Finally, abstract machine executes the program proc y^* ; do $s^\#$. The synchronization check is exposed to the user, who invokes the abstract machine interpreter with concrete integer values corresponding to the control variables y^* . The control-value environment $\sigma : \mathbb{Y} \rightarrow \mathbb{Z}$ is initialized based on the user's input. The statement $s^\#$ is then evaluated according to the semantics defined previously. Note that the task id ι is initialized to 0, and the synchronization ρ is initially empty.

6 PERFORMANCE RESULTS

We implemented tf32-precision GEMM kernels for the sm_90a architecture, using wmma and TMA instructions. We also implemented a full-precision fp32 GEMV kernel using warp shuffles and scalar math [12]; this did not use the accelerator instructions. We compared the Exo-GPU kernels to cuBLAS's cublasSgemm, cublasSgemmStridedBatched, and cublasSgemv functions, all with the

834 math mode set to CUBLAS_TF32_TENSOR_OP_MATH. Our sm_90a-compatible test hardware contained
 835 an NVIDIA H100 80GB SXM5 GPU and an AMD EPYC 9454 48-Core Processor, and we used nvcc
 836 Build cuda_12.3.r12.3/compiler.33492891_0 to compile the CUDA C++ sources generated
 837 by Exo-GPU. For GEMM, a compute-bound workload, theoretical peak is 494.5 TFLOPS [17]. For
 838 GEMV, a memory-bound workload, we derive the theoretical peak from the memory bandwidth:
 839 $3.35 \frac{\text{TB}}{\text{s}} \frac{2 \text{ FLOP}}{4 \text{ B}} = 1.675 \frac{\text{TFLOP}}{\text{s}}$, with one multiply and one add done for each 4 byte tf32 element loaded
 840 from the matrix (the bandwidth from loading the vector is amortized).

841 We tested each problem size and hardware combination over 105 iterations: 5 warm-up iterations,
 842 and 100 timed iterations, with the pcg3d hash algorithm [9] used to generate “random” input
 843 matrices. Each iteration tested, in a randomized order, the cubLAS kernel and all applicable Exo-
 844 GPU kernel variants for that problem size. In particular, we tested non-split-k and split-k variants of
 845 the GEMM kernel, with the split-k kernels using cp.reduce.async.bulk (TMA) and split factors
 846 of 1, 2, 4, 8, and 16. For each (problem size, hardware) combination, we collected 100 time samples
 847 per tested kernel and reported the mean of the inter-quartile range (middle 50 samples). For each
 848 plot in Figure 8, we report the best-performing Exo-GPU kernel for each problem size (plotted as
 849 “Exo-GPU (specialized)”) and the single best-performing Exo-GPU kernel (“Exo-GPU (one kernel)”).

850 For large, square matrix GEMM problem sizes, we see very similar performance between Exo-
 851 GPU and CUBLAS; this is expected, as Exo-GPU is able to express all optimizations required for a
 852 peak-performance sm_90a gemm: warp specialization, cluster & TMA multicast support, wmma
 853 support, and split-barrier synchronization using commit group, mbarrier, and cluster sync mecha-
 854 nisms. For more unusual GEMM problem sizes, such as small matrices and K=65536 workloads,
 855 we see more variation between Exo-GPU and CUBLAS, possibly due to different problem size
 856 thresholds for observing wave quantization effects. For GEMV, Exo-GPU and CUBLAS follow a
 857 similar performance trend, with CUBLAS having an almost-consistent performance advantage.

858 **Abstract Machine performance.** We re-
 859 port the performance of the synchronization
 860 checking alone, which is implemented as an
 861 interpreter for the abstract machine (Section 5).
 862 We benchmarked using only one thread of a laptop
 863 with an “11th Gen Intel(R) Core(TM)
 864 i7-11850H @ 2.50GHz” CPU. In Figure 9, we
 865 report times for concrete square matrix prob-
 866 lem sizes for the GEMV kernel and the sm_90a
 867 GEMM kernel described earlier (both the split-k
 868 and non-split-k versions). The batch size L is 1.
 869 We use one untimed warmup run for each prob-
 870 lem size, and report the average of five timed
 871 runs, as reported by the timeit module of Python 3.10.12.

872 We observe that runtimes are linear in the number of memory operations interpreted. The
 873 number of memory operations is cubic in the problem size for GEMM, and quadratic for GEMV.
 874 We see this pattern followed cleanly by the measured trend (e.g. 2/16/128 seconds for GEMM for
 875 1024/2048/4096 problem size), indicating no unexpected overhead for large problem sizes. The
 876 bump for small GEMM problem sizes is due to imperfect division by the per-cluster tile size. Even if
 877 the expected problem size for a deployed kernel is large, during development of an Exo-GPU kernel,
 878 it generally suffices to test only with a small problem size (e.g. 768) for immediate feedback on
 879 bugs, with the option of testing the finalized kernel with the true, larger problem size for additional
 880 confidence.

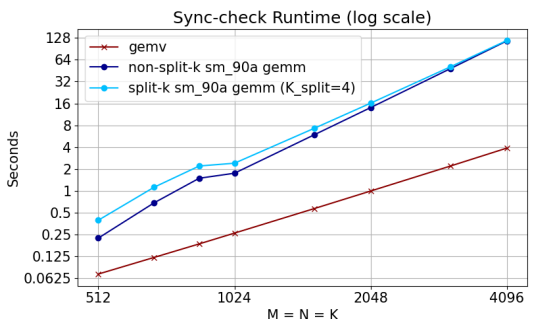


Fig. 9. Sync-check runtime by problem size.

883 7 RELATED WORK

884 7.1 GPU Kernel Authoring Languages

885 While CUDA offers fine-grained control, it remains low-level and error-prone. To address this,
 886 various approaches have emerged at different abstraction levels.
 887

888 *Higher-level abstractions:* Tile-level DSLs like Triton [24] and Pallas [1] abstract away low-
 889 level details by enabling programmers to express computations at the block level, with compilers
 890 automatically handling the thread-level mapping. However, these abstractions can hide performance-
 891 critical details. When Triton performance fell far behind state-of-the-art for Blackwell GPUs, they
 892 had to invent Gluon, a lower-level language that gives users direct control over tile layouts, memory
 893 allocation, data movement, and asynchrony, essentially abandoning the higher-level automation
 894 to regain the fine-grained control necessary for peak performance. Rather than starting with
 895 automation that may later prove inadequate, Exo-GPU deliberately maintains a thin abstraction
 896 layer over CUDA. Performance-critical constructs, including control flow and data copies across
 897 the memory hierarchy, are made explicit statements in Exo-GPU’s imperative object code.

898 *Template-based libraries:* CUTLASS [15] and ThunderKittens [22] are C++ template-based li-
 899 braries that raise the abstraction of GPU programming while preserving performance. Instead of
 900 hiding CUDA behind rigid abstractions, they provide composable, architecture-aware primitives
 901 that integrate with raw CUDA code. This approach lets programmers work at the tile level when
 902 convenient, yet seamlessly drop to thread-level operations when fine control is needed. CuTe [14],
 903 introduced in CUTLASS 3.0, offers flexible abstraction for defining tensor layouts and transforma-
 904 tions. While these libraries are effective engineering toolkits, they do not provide safety guarantees
 905 or whole-program analyses for asynchronous instructions and synchronization statements.

906 Achieving both peak performance and safety remains a fundamental challenge. Existing ap-
 907 proaches either provide limited safety guarantees or lack support for modern GPU features. For
 908 instance, Descend [11] introduces Rust-like borrow checking to ensure race freedom but does not
 909 support key GPU features such as tensor cores and split barriers. The aforementioned tile- and
 910 template-based languages are practical tools, yet do not offer safety guarantees. This motivated the
 911 collective analysis (Section 4) and synchronization checking via abstract machine (Section 5).

912 7.2 User-schedulable Languages

913 User-schedulable languages (USLs) describe optimization as rewriting programs into new pro-
 914 grams that compute the same result, but execute much faster. Rather than relying on opaque
 915 compiler heuristics, programmers directly control these rewrites by specifying scheduling oper-
 916 ations. Halide [19, 20] popularized the idea of USLs, and subsequent Halide-inspired languages
 917 explored different target applications and abstraction for a given domain [2, 3, 5–7, 10, 23, 25, 26, 28].
 918 For instance, TVM offers accelerator abstraction through `tensorize`, TACO separates tensor defi-
 919 nitions from sparse formats, and Taichi abstracts memory layout and management with `fields`.
 920

921 Several systems have extended user-scheduling to support modern GPU features. TVM’s Ten-
 922 sorIR [4] provides intrinsics for manipulating low-level constructs like split barriers, while Cy-
 923 press [27] lets programmers describe computations as tasks and map them to different resources.
 924 Exo-GPU differs from these approaches in two key ways. First, Exo-GPU exposes low-level control
 925 to the programmer; there is little hidden control flow in GPU IR. In this sense, Exo-GPU follows a
 926 WYSIWYG (what you see is what you get) philosophy: the structure of the program directly reflects
 927 its execution. This contrasts with Cypress, which hides warp specialization as an internal com-
 928 piler optimization, and with TensorIR, which focuses on automatically generating schedules with
 929 lowering-based intrinsics. Second, Exo-GPU guarantees sequential-parallel equivalence through a
 930 synchronization checker that detects data races, hazards, and other concurrency bugs.

932

7.3 Exo vs. Exo-GPU

933 Exo-GPU fundamentally extends existing the Exo language by introducing parallel semantics. While
 934 Exo [7, 8] is a high-performance USL that achieves peak performance on many vector machines
 935 and accelerators, it was designed to exploit only the *implicit parallelism* exposed by hardware.
 936 Exo’s scheduling reasoning operates exclusively under a sequential execution model. This approach
 937 suffices for vector machines and matrix accelerators because CPU frontends maintain instruction
 938 ordering; even with out-of-order execution and reorder buffers, the hardware guarantees that
 939 parallel execution produces results equivalent to sequential execution. Therefore, the compiler
 940 needs only to verify program equivalence when interpreting object code sequentially. Even within
 941 this sequential framework, Exo’s optimizations could exploit implicit hardware parallelism through
 942 techniques like software pipelining [7, 8].

943 In contrast, GPUs expose *explicit data- and instruction-parallelism* to software. Unlike traditional
 944 CPUs and accelerators that maintain the illusion of sequential execution through their frontend,
 945 modern GPUs shift this responsibility entirely to software. For Exo, this shift requires reasoning
 946 about parallel execution at the object code level and establishing equivalence not just within
 947 programming models, but across sequential and parallel paradigms. We address this fundamental
 948 challenge through two key contributions. First, we extend Exo’s object code and scheduling language
 949 to expose user-controlled parallel loops and synchronization features. Second, we provide safety
 950 guarantees by establishing sequential-parallel equivalence through the abstract machine. This
 951 completes the equivalence chain from the simple, initial Exo program through to its optimized,
 952 parallel implementation in Exo-GPU, ensuring correctness at every transformation step.
 953

954
955

8 LIMITATIONS AND FUTURE WORK

956 To optimize Hopper GEMMs (Figure 8), we had to apply two
 957 rewrite steps that were out-of-scope of Exo’s sequential safety
 958 checks. These patterns arise when modeling TMA’s asynchronous
 959 copy instruction, which supports default behavior for out-
 960 of-bounds reads and writes. Inset right figure shows a minimal
 961 example that illustrates the problem. Even though removing the
 962 first guard is safe since the `tmp[6]` and `tmp[7]` are not being read by C in the second loop thanks to
 963 the guard, Exo’s dependency-based checks treat these writes as semantically relevant and cannot
 964 prove they are observationally redundant. We marked these transformations as *unsafe* in our sched-
 965 ules, despite being semantically sound. To address this issue, we need to extend Exo’s sequential
 966 scheduling rewrites with value-sensitivity.
 967

968 Our ability to reason about parallelism is incomplete in several ways. Our programming model
 969 and output CUDA synchronization code is generated based on our understanding of PTX as
 970 documented by NVIDIA in natural language [18]. We do not show that our generated code is
 971 correct with respect to any formal CUDA semantics. We currently do not support Blackwell
 972 Tensor Cores (tcgen05), nor do we support platforms not providing CUDA C++ and inline PTX
 973 support. Finally, our current synchronization checking approach – translation to abstract machine
 974 IR followed by software interpretation – supports only concrete problem sizes and limits compiler
 975 performance. This approach may be improved with static analysis of the abstract machine program.
 976

977 Nevertheless, we believe that our approach—exposing detailed control to programmers while
 978 verifying its safety—offers a promising path forward for GPU programming. By treating parallelism
 979 and synchronization as analyzable annotations on sequential code, Exo-GPU provides both the
 transparency and static guarantees that high-performance GPU kernels demand.

```
tmp : f32[8] @ tmp_mem
for i in seq(0, 8):
    if i < 6: # removing is safe
        tmp[i] = 0
    for i in seq(0, 8):
        if i < 6:
            C[i] = tmp[i]
```

981 REFERENCES

- [1] The JAX authors. 2024. Pallas: a JAX kernel language. <https://docs.jax.dev/en/latest/pallas/index.html>
- [2] Michael Bauer, Sean Treichler, Elliott Slaughter, and Alex Aiken. 2012. Legion: expressing locality and independence with logical regions. In *SC Conference on High Performance Computing Networking, Storage and Analysis, SC '12* (Salt Lake City, UT, USA). IEEE, Piscataway, NJ, USA, 66. <https://doi.org/10.1109/SC.2012.71>
- [3] Tianqi Chen, Thierry Moreau, Ziheng Jiang, Lianmin Zheng, Eddie Yan, Meghan Cowan, Haichen Shen, Leyuan Wang, Yuwei Hu, Luis Ceze, Carlos Guestrin, and Arvind Krishnamurthy. 2018. TVM: An Automated End-to-end Optimizing Compiler for Deep Learning. In *Proceedings of the 12th USENIX Conference on Operating Systems Design and Implementation* (Carlsbad, CA, USA) (OSDI'18). USENIX Association, Berkeley, CA, USA, 579–594. <http://dl.acm.org/citation.cfm?id=3291168.3291211>
- [4] Siyuan Feng, Bohan Hou, Hongyi Jin, Wuwei Lin, Junru Shao, Ruihang Lai, Zihao Ye, Lianmin Zheng, Cody Hao Yu, Yong Yu, and Tianqi Chen. 2023. TensorIR: An Abstraction for Automatic Tensorized Program Optimization. In *Proceedings of the 28th ACM International Conference on Architectural Support for Programming Languages and Operating Systems, Volume 2* (Vancouver, BC, Canada) (ASPLOS 2023). Association for Computing Machinery, New York, NY, USA, 804–817. <https://doi.org/10.1145/3575693.3576933>
- [5] Bastian Hagedorn, Archibald Samuel Elliott, Henrik Barthels, Rastislav Bodík, and Vinod Grover. 2020. Fireiron: A Data-Movement-Aware Scheduling Language for GPUs. In *PACT '20: International Conference on Parallel Architectures and Compilation Techniques, Virtual Event, GA, USA, October 3–7, 2020*. Vivek Sarkar and Hyesoon Kim (Eds.). ACM, 71–82. <https://doi.org/10.1145/3410463.3414632>
- [6] Yuanning Hu, Tzu-Mao Li, Luke Anderson, Jonathan Ragan-Kelley, and Frédo Durand. 2019. Taichi: a language for high-performance computation on spatially sparse data structures. *ACM Trans. Graph.* 38, 6 (2019), 201:1–201:16. <https://doi.org/10.1145/3355089.3356506>
- [7] Yuka Ikarashi, Gilbert Louis Bernstein, Alex Reinking, Hasan Genc, and Jonathan Ragan-Kelley. 2022. Exocompilation for Productive Programming of Hardware Accelerators. In *Proceedings of the 43rd ACM SIGPLAN International Conference on Programming Language Design and Implementation* (San Diego, CA, USA) (PLDI 2022). Association for Computing Machinery, New York, NY, USA, 703–718. <https://doi.org/10.1145/3519939.3523446>
- [8] Yuka Ikarashi, Kevin Qian, Samir Droubi, Alex Reinking, Gilbert Louis Bernstein, and Jonathan Ragan-Kelley. 2025. Exo 2: Growing a Scheduling Language. In *Proceedings of the 30th ACM International Conference on Architectural Support for Programming Languages and Operating Systems, Volume 1* (Rotterdam, Netherlands) (ASPLOS '25). Association for Computing Machinery, New York, NY, USA, 426–444. <https://doi.org/10.1145/3669940.3707218>
- [9] Mark Jarzynski and Marc Olano. 2020. A PCC3D Family of Hash Functions. <https://github.com/markjarzynski/PCC3D>
- [10] Fredrik Kjolstad, Shoaib Kamil, Stephen Chou, David Lugato, and Saman Amarasinghe. 2017. The tensor algebra compiler. *Proceedings of the ACM on Programming Languages* 1, OOPSLA (oct 2017), 1–29. <https://doi.org/10.1145/3133901>
- [11] Bastian Köpcke, Sergei Gorlatch, and Michel Steuwer. 2024. Descend: A Safe GPU Systems Programming Language. *Proc. ACM Program. Lang.* 8, PLDI, Article 181 (June 2024), 24 pages. <https://doi.org/10.1145/3656411>
- [12] Bruce Lee. 2024. CUDA HGEMV. https://github.com/Bruce-Lee-LY/cuda_hgemv
- [13] NVIDIA. 2017. NVIDIA Tesla V100 GPU Architecture. <https://images.nvidia.com/content/volta-architecture/pdf/volta-architecture-whitepaper.pdf>
- [14] NVIDIA. 2025. CuTe. <https://docs.nvidia.com/cutlass/media/docs/cpp/cute>
- [15] NVIDIA. 2025. CUTLASS 4.2.1. <https://github.com/NVIDIA/cutlass>
- [16] NVIDIA. 2025. CUTLASS grouped kernel schedules. https://docs.nvidia.com/cutlass/media/docs/cpp/grouped_scheduler.html
- [17] NVIDIA. 2025. H100 GPU. <https://www.nvidia.com/en-us/data-center/h100/>
- [18] NVIDIA. 2025. Parallel Thread Execution ISA Version 9.0. <https://docs.nvidia.com/cuda/parallel-thread-execution/>
- [19] Jonathan Ragan-Kelley, Andrew Adams, Sylvain Paris, Marc Levoy, Saman P. Amarasinghe, and Frédo Durand. 2012. Decoupling algorithms from schedules for easy optimization of image processing pipelines. *ACM Trans. Graph.* 31, 4 (2012), 32:1–32:12. <https://doi.org/10.1145/2185520.2185528>
- [20] Jonathan Ragan-Kelley, Andrew Adams, Dillon Sharlet, Connelly Barnes, Sylvain Paris, Marc Levoy, Saman P. Amarasinghe, and Frédo Durand. 2018. Halide: decoupling algorithms from schedules for high-performance image processing. *Commun. ACM* 61, 1 (2018), 106–115. <https://doi.org/10.1145/3150211>
- [21] Jay Shah, Ganesh Bikshandi, Ying Zhang, Vijay Thakkar, Pradeep Ramani, and Tri Dao. 2024. FlashAttention-3: Fast and Accurate Attention with Asynchrony and Low-precision. arXiv:2407.08608 [cs.LG] <https://arxiv.org/abs/2407.08608>
- [22] Benjamin F. Spector, Simran Arora, Aaryan Singhal, Daniel Y. Fu, and Christopher Ré. 2024. ThunderKittens: Simple, Fast, and Adorable AI Kernels. arXiv:2410.20399 [cs.LG] <https://arxiv.org/abs/2410.20399>
- [23] Michel Steuwer, Toomas Remmelg, and Christophe Dubach. 2017. LIFT: A functional data-parallel IR for high-performance GPU code generation. In *2017 IEEE/ACM International Symposium on Code Generation and Optimization*

- 1030 (CGO). IEEE, Piscataway, NJ, USA, 74–85. <https://doi.org/10.1109/CGO.2017.7863730>
- 1031 [24] Philippe Tillet, H. T. Kung, and David Cox. 2019. Triton: an intermediate language and compiler for tiled neural
1032 network computations. In *Proceedings of the 3rd ACM SIGPLAN International Workshop on Machine Learning and
1033 Programming Languages* (Phoenix, AZ, USA) (MAPL 2019). Association for Computing Machinery, New York, NY,
1034 USA, 10–19. <https://doi.org/10.1145/3315508.3329973>
- 1035 [25] Nicolas Vasilache, Oleksandr Zinenko, Theodoros Theodidis, Priya Goyal, Zachary DeVito, William S. Moses,
1036 Sven Verdoolaege, Andrew Adams, and Albert Cohen. 2018. Tensor Comprehensions: Framework-Agnostic High-
1037 Performance Machine Learning Abstractions. arXiv:1802.04730 [cs.PL]
- 1038 [26] Anand Venkat, Tharindu Rusira, Raj Barik, Mary Hall, and Leonard Truong. 2019. SWIRL: High-performance many-
1039 core CPU code generation for deep neural networks. *The International Journal of High Performance Computing
1040 Applications* 33, 6 (2019), 1275–1289. <https://doi.org/10.1177/1094342019866247>
- 1041 [27] Rohan Yadav, Michael Garland, Alex Aiken, and Michael Bauer. 2025. Task-Based Tensor Computations on Modern
1042 GPUs. *Proc. ACM Program. Lang.* 9, PLDI, Article 163 (June 2025), 25 pages. <https://doi.org/10.1145/3729262>
- 1043
- 1044
- 1045
- 1046
- 1047
- 1048
- 1049
- 1050
- 1051
- 1052
- 1053
- 1054
- 1055
- 1056
- 1057
- 1058
- 1059
- 1060
- 1061
- 1062
- 1063
- 1064
- 1065
- 1066
- 1067
- 1068
- 1069
- 1070
- 1071
- 1072
- 1073
- 1074
- 1075
- 1076
- 1077
- 1078

1079 A GPU IR TYPE DEFINITIONS

1081	$\tau_x : \text{DataType} ::= \text{f32}$	32-bit floating point
1082	f64	64-bit floating point
1083	f16	16-bit floating point
1084	i32	32-bit integer
1085	ui16	16-bit unsigned integer
1086	i8	8-bit integer
1087	ui8	8-bit unsigned integer
1088	$\tau_z : \text{BarrierType} ::= \text{barrier}$	non-explicitly guarded barrier
1089		$\text{barrier}(z)$ explicitly guarded barrier

1090 Fig. 10. List of variable types

1091
1092

		domain	box
1094	$\tau_u : \text{CollUnit} ::= \text{standalone_thread}$	(1,)	(1,)
1095	$n_1 * \text{cuda_thread}$	(blockDim,)	(n ₁ ,)
1096	cuda_quadpair	(blockDim/16, 16)	(2, 4)
1097	$n_1 * \text{cuda_warp}$	(blockDim,)	(n ₁ * 32,)
1098	$n_1 * \text{cuda_warpgroup}$	(blockDim,)	(n ₁ * 128,)
1099	$n_1 * \text{cuda_threads_strided}(n_2, n_3)$	(blockDim/n ₃ , n ₃)	(n ₁ , n ₂)
1100	$n_1 * \text{cuda_warp_in_cluster}$	(clusterDim, blockDim)	(n ₁ , 32)
1101	$n_1 * \text{cuda_cta_in_cluster}$	(clusterDim * blockDim,)	(n ₁ * blockDim,)
1102	cuda_cluster	(clusterDim * blockDim,)	(clusterDim * blockDim,)
1103	$n_1 * \text{cuda_cta_in_cluster_strided}(n_3)$	(ClusterDim/n ₃ , n ₃ , blockDim)	(n ₁ , 1, blockDim)
1104	$n_1 * \text{cuda_warp_in_cluster_strided}(n_3)$	(clusterDim/n ₃ , n ₃ , blockDim)	(n ₁ , 1, 32)
1105	$\text{cuda_agnostic_sub_cta}$	(clusterDim, blockDim)	(1, _)
	$\text{cuda_agnostic_intact_cta}$	(clusterDim, blockDim)	(_, blockDim)

1106 Fig. 11. Collective units defined in the frontend language. These are parameterized by a collective type δ ,
1107 which consists of the *domain* and *box* shown here.1108
1109

1110	$\pi_d : \text{DataMemory} ::= \text{CudaBasicDeviceVisible}$	base type for CUDA-visible allocations
1111	CudaBasicSmem	base type for CUDA SMEM allocations
1112	CudaDeviceVisibleAtomicity16B	base type for 16B-atomicity layout CUDA-visible allocations
1113	CudaDeviceVisibleLinear	base type for linear-order CUDA-visible allocations
1114	CudaGridConstant	CUDA grid constant memory
1115	CudaGmemLinear	CUDA global memory, linear-order
1116	CudaSmemAtomicity16B	Any CUDA shared memory with 16B-atomicity layout
1117	CudaSmemLinear	CUDA shared memory with linear-order layout
1118	CudaRmem	Per-thread CUDA registers
1119	Sm80_RmemMatrixA(M, K)	Matrix tile for sm_80+ warp MMA A operand
1120	Sm80_RmemMatrixB(N, K)	Matrix tile for sm_80+ warp MMA B operand
1121	Sm80_RmemMatrixD(M, N)	Matrix tile for sm_80+ MMA accumulator operands
1122	Sm90_SmemSwizzled(B)	B-byte swizzled shared memory, in TMA/wmma-accepted format
1123	Sm90_RmemMatrixA(M)	Register tile for wmma A operand (not implemented)
	Sm90_RmemMatrixD(M, N)	Register tile for wmma D operand

1124 Fig. 12. CUDA Memory Types – Data Allocations (pre-existing Exo Memory not listed)

1125
1126
1127

```

1128  $\pi_z : \text{BarrierComp} ::= \text{CudaDeviceBarrier}$  base type for CUDA-allocated barriers
1129 | CudaMbarrier CUDA mbarrier
1130 | CudaCommitGroup CUDA commit_group mechanism
1131 | CudaClusterSync barrier.cluster sync

```

Fig. 13. CUDA Barrier (completion) mechanisms

```

1135  $\pi_w : \text{SpecialWindow} ::= \text{Sm90\_tensorMap(swizzle, *smem\_box)}$  CUtensorMap parameterized by swizzle mode and box size
1136

```

Fig. 14. CUDA Special Window Types (for Window Statement)

$\tau_q : \text{QualTL} ::= \text{cpu_in_order_qual}$	Ordinary CPU reads/writes (cpu)
$\text{cpu_cuda_stream_qual}$	Stream-ordered CUDA API calls (strm)
$\text{cuda_in_order_rmem_qual}$	non-asynchronous CUDA instrs' accesses to registers (cuda1)
$\text{cuda_in_order_ram_qual}$	non-asynchronous CUDA instrs' accesses to SMEM/GMEM (cuda2)
$\text{Sm80_cp_async_qual}$	non-bulk cp.async memory accesses (Sm80)
$\text{tma_to_smem_async_qual}$	cp.async.bulk GMEM reads, SMEM writes (tmaS)
$\text{tma_to_gmem_async_qual}$	cp.async.bulk SMEM reads, GMEM writes/reduces (tmaG)
$\text{wmma_async_rmem_a_qual}$	wmma.mma_async reads from A register parameter (wgA)
$\text{wmma_async_rmem_d_qual}$	wmma.mma_async accesses to D (accumulator) (wgD)
$\text{wmma_async_smem_qual}$	wmma.mma_async access to SMEM, A or B (wgS)
wmma_zero_qual	special case used to model the wmma scale-d parameter (wg0)

Fig. 15. List of qualitative timelines

$\tau_s : \text{SyncTL}$	trnstv?	cpu	strm	cuda1	cuda2	Sm80	tmaS	tmaG	wgA	wgD	wgS	wg0
empty_sync_tl												
cpu_in_order	y	full										
cuda_stream_sync	y		full									
cuda_in_order	y		temp.	full	full	temp.						
cuda_temporal			temp.									
Sm80_cp_async						full						
Sm80_generic						full	temp.	temp.	temp.	temp.	temp.	temp.
tma_to_smem_async							temp.	temp.	temp.	temp.	temp.	temp.
tma_to_gmem_async							full	full	full	full	full	full
wmma_async_smem												full
wmma_fence_1									full	full		
wmma_fence_2									full	full		
wmma_async									full	full	full	
cuda_async_proxy										full		
cuda_async_proxy_wmma									full	full	full	
cuda_generic_and_async		temp.	full	full		full	full	full	temp.	temp.	full	temp.

Fig. 16. SyncTL are defined as composition of QualTL.

B ABSTRACT MACHINE CONVERSION AND SEMANTICS DEFINITIONS

A new record Constructor \mathcal{R} is used to define RecordRead and RecordMutate in Figure 22. RECORDREAD and RECORDMUTATE first evaluate the accessor $e^\#$ and $e_z^\#$ to access sets $W_{e^\#}$ and $W_{e_z^\#}$ (via \Downarrow_{Acc}). They then update the visibility map ρ at each key $(x, n) \in W_{e^\#}$ using the new record constructor \mathcal{R} defined below: RECORDREAD adds it to the *read* visibility set, setting $\rho'(x, n).r = \rho(x, n).r \cup \mathcal{R}(\dots)$ while leaving $\rho(x, n).m$ and $\rho(x, n).b$ unchanged; RECORDMUTATE adds it to the *mutate* visibility

1177 set, setting $\rho'(x, \mathbf{n}).m = \rho(x, \mathbf{n}).m \cup \mathcal{R}(\dots)$ while preserving $\rho(x, \mathbf{n}).r$ and $\rho(x, \mathbf{n}).b$. In both cases,
 1178 neither the control i nor the store σ changes.

1179 **Definition B.1** (New Record Constructor \mathcal{R}). Define \mathcal{R} as follows:

$$1180 \quad \mathcal{R} : VL \times Bool \times QualTL \times \mathcal{P}(QualTL) \times Expr^\# \times \rho \times \mathbb{G} \longrightarrow \mathcal{P}(\mathbb{R})$$

$$1182 \quad \mathcal{R}(\tau_v, t, \tau_q, \tau_q^*, E^\#, \rho, G) = \begin{cases} \{(\tau_q, S_G, P_{E^\#, \rho})\}, & t = \text{true}, \\ \{(\tau_q, S_{\{g\}}, P_{E^\#, \rho}) \mid g \in G\}, & t = \text{false}, \end{cases}$$

1185 where, for any $H \subseteq \mathbb{G}$, $S_H \in \mathbb{S}$ and $P_{E^\#, \rho} \in \mathbb{P}$ are given pointwise by

$$1187 \quad S_H(g', \tau_q') = \max_{VL} \left(\begin{cases} \text{atomic_only}, & \tau_q' \in \tau_q^*, \\ \text{invisible}, & \text{otherwise} \end{cases}, \begin{cases} \tau_v, & g' \in H \wedge \tau_q' = \tau_q, \\ \text{invisible}, & \text{otherwise} \end{cases} \right),$$

$$1190 \quad P_{E^\#, \rho}(z, \mathbf{n}) = \begin{cases} \{a\}, & (z, \mathbf{n}) \in E^\# \text{ where } (a, _) = \rho(z, \mathbf{n}).b, \\ \emptyset, & \text{otherwise}. \end{cases}$$

1192 Fence, Arrive, and Await (Figure 22) update ρ solely via $\text{lift}(\rho, \lambda)$ (defined below), which applies
 1193 λ pointwise to both the read and mutate visibility sets. For $\text{Fence}(t, \tau_q^{\text{pre}*}, \tau_q^{\text{full}*}, \tau_q^{\text{temp}*})$, $\lambda(r) =$
 1194 $\mathcal{A}(r, g^{\text{exec}*}, \tau_q^{\text{full}*}, \tau_q^{\text{temp}*})$ iff the witness $\mathcal{W}(t, g^{\text{exec}*}, \tau_q^{\text{pre}*}, r)$ holds, otherwise $\lambda(r) = r$; thus
 1195 visibility is raised by joining $f \vee f_{\text{aug}}$. For $\text{Arrive}(t, \tau_q^{\text{pre}*}, e_z^{\#*})$, the accessed sets yield a unique
 1196 home barrier $\{(z, \mathbf{n})\} = \bigcap_i W_{e_z^{\#*}}$; guarded by \mathcal{W} , λ adds the existing arrive count a from $\rho(z, \mathbf{n})$
 1197 into $r.p$ at every $(z, \mathbf{n}) \in \mathbf{W}$, and home barrier's arrive count is incremented by $(a' + 1, w')$.
 1198 For $\text{Await}(e_z^{\#*}, \tau_q^{\text{full}*}, \tau_q^{\text{temp}*}, n)$, with $(a, w) = \rho(z, \mathbf{n}).b$, compute Max and New as in the rule; set
 1199 $\lambda(r) = \mathcal{A}(r, g_s^*(\rho), \tau_q^{\text{full}*}, \tau_q^{\text{temp}*})$ iff some observed arrive count $i \in r.p(z, \mathbf{n})$ satisfies $i \leq \text{Max}$,
 1200 else $\lambda(r) = r$; after lift, update the wait count to (a', New) . In short, \mathcal{W} decides when augmentation
 1201 is permitted, \mathcal{A} raises visibility to fully_ordered or temporally_ordered.

1204 **Definition B.2** (Lift). For $\lambda : \mathbb{R} \rightarrow \mathbb{R}$, define $\text{lift}(\rho, \lambda)$ pointwise by

$$1205 \quad \text{lift}(\rho, \lambda)(x, v) = (\{\lambda(r) \mid r \in R\}, \{\lambda(r) \mid r \in M\}, (a, w)) \quad \text{where } (R, M, (a, w)) = \rho(x, v).$$

1207 **Definition B.3** (Synchronization helpers). Let $r = (\tau_q^{\text{orig}}, \mathcal{f}, p) \in \mathbb{R}$ with $\mathcal{f} \in \mathbb{S}$. For $\mathcal{f}_1, \mathcal{f}_2 \in \mathbb{S}$, define
 1208 the pointwise join $(\mathcal{f}_1 \vee \mathcal{f}_2)(g, \tau_q) = \max_{VL} \{\mathcal{f}_1(g, \tau_q), \mathcal{f}_2(g, \tau_q)\}$.

1209 (i) *Witness \mathcal{W}* . For $t \in \text{Bool}$, $g^{\text{exec}*} \subseteq \mathbb{G}$, and $\tau_q^{\text{pre}*} \subseteq \text{QualTL}$, set

$$1211 \quad \mathcal{W}(t, g^{\text{exec}*}, \tau_q^{\text{pre}*}, r) = \begin{cases} \exists g \in g^{\text{exec}*} \exists \tau_q \in \tau_q^{\text{pre}*} : \mathcal{f}(g, \tau_q) \geq \text{unordered}, & t = \text{true}, \\ (\tau_q^{\text{orig}} \in \tau_q^{\text{pre}*}) \wedge \exists g \in g^{\text{exec}*} : \mathcal{f}(g, \tau_q^{\text{orig}}) \geq \text{unordered}, & t = \text{false}. \end{cases}$$

1214 (ii) *Augment \mathcal{A}* . Given $g^{\text{exec}*} \subseteq \mathbb{G}$ and $\tau_q^{\text{full}*}, \tau_q^{\text{temp}*} \subseteq \text{QualTL}$, define

$$1215 \quad \mathcal{A}(r, g^{\text{exec}*}, \tau_q^{\text{full}*}, \tau_q^{\text{temp}*}) = (\tau_q^{\text{orig}}, \mathcal{f} \vee \mathcal{f}_{\text{aug}}, p),$$

$$1217 \quad \mathcal{f}_{\text{aug}}(g, \tau_q) = \begin{cases} \text{fully_ordered}, & g \in g^{\text{exec}*} \wedge \tau_q \in \tau_q^{\text{full}*}, \\ \text{temporally_ordered}, & g \in g^{\text{exec}*} \wedge \tau_q \in \tau_q^{\text{temp}*} \setminus \tau_q^{\text{full}*}, \\ \text{invisible}, & \text{otherwise}. \end{cases}$$

1221

1222

1223

1224

1225

	<i>Data expressions</i> $e \in \text{DExpr}$	$\mathcal{P}(\text{Expr}^\#)$
1226	d	\emptyset
1227	x	$\{x[\langle\rangle]\}$
1228	$x[w^*]$	$\{x[w^*]\}$
1229	$e_1 \text{ op } e_2 \quad (\text{op} \in \{+, -, *, /\})$	$T_e(e_1) \cup T_e(e_2)$
1230	<hr/>	
1231	<i>Barrier expressions</i> $e_z \in \text{ZExpr}$	
1232	z	$\{z[\langle\rangle]\}$
1233	$z[w^*]$	$\{z[w^*]\}$
1234	<hr/>	
1235		

Fig. 17. Expression conversion $T_e : \text{DExpr} \cup \text{ZExpr} \rightarrow \mathcal{P}(\text{Expr}^\#)$ collects the distinct reads in an expression and returns them as a set of AMIR reads ($\text{Expr}^\#$).

	Type	Definition
1240	$T_{\text{smem}} : \text{Expr} \rightarrow \mathcal{P}(\text{Expr}^\#)$	$T_{\text{smem}}(e) \triangleq \{e^\# \in T_e(e) \mid \text{isSmem}(e^\#)\}.$
1241	$T_{\text{ex}} : \text{Expr} \rightarrow \mathcal{P}(\text{Expr}^\#)$	$T_{\text{ex}}(e) \triangleq \{e^\# \in T_e(e) \mid \neg \text{isEx}(e^\#)\}.$
1242	$\text{isEx} : \text{Expr}^\# \rightarrow \text{Bool}$	$\text{isEx}(e^\#) \triangleq \text{true iff } e^\# \text{ is annotated as sync-exempt memory; false otherwise.}$
1243	$\text{isSmem} : \text{Expr}^\# \rightarrow \text{Bool}$	$\text{isSmem}(e^\#) \triangleq \text{true iff } e^\# \text{ is annotated as shared memory; false otherwise.}$
1244	$T_{\text{tr}} : \text{SyncTL} \rightarrow \text{Bool}$	$T_{\text{tr}}(\tau_s) \triangleq \text{true iff } \tau_s \text{ is transitive; false otherwise.}$
1245	$T_{\text{qfull}} : \text{SyncTL} \rightarrow \mathcal{P}(\text{QualTL})$	$T_{\text{qfull}}(\tau_s) \triangleq \{\tau'_q \in \text{QualTL} \mid \tau'_q \text{ annotated as "full" in } \tau_s\}.$
1246	$T_{\text{qtmp}} : \text{SyncTL} \rightarrow \mathcal{P}(\text{QualTL})$	$T_{\text{qtmp}}(\tau_s) \triangleq \{\tau'_q \in \text{QualTL} \mid \tau'_q \text{ annotated as "temporal" or "full" in } \tau_s\}.$
1247	$T_{\text{qarr}} : \text{SyncTL} \rightarrow \text{QualTL}$	$T_{\text{qarr}}(\tau_s) \triangleq \begin{cases} \text{Sm80_cp_async_qual}, & \text{if Sm80_cp_async_qual} \in T_{\text{qfull}}(\tau_s), \\ \text{cuda_in_order_qual}, & \text{otherwise.} \end{cases}$
1248	$T_{\text{qin}} : \text{Expr}^\# \rightarrow \text{QualTL}$	$T_{\text{qin}}(e^\#) \triangleq \begin{cases} \text{cpu_in_order_qual}, & \text{if } e^\# \text{ is host/CPU scoped,} \\ \text{cuda_in_order_rmem_qual}, & \text{if } e^\# \text{ is register memory,} \\ \text{cuda_in_order_ram_qual}, & \text{otherwise.} \end{cases}$
1249	<hr/>	
1250		
1251		
1252		
1253		
1254		

Fig. 18. Helper functions used by Fig. 5 statement conversion. All sets are finite.

1255
1256
1257
1258
1259
1260
1261
1262
1263
1264
1265
1266
1267
1268
1269
1270
1271
1272
1273
1274

1275	Case for $g.p_i$	Abstract Machine IR
1276	Non-atomic <i>read-only</i>	$\vdots_{e^\# \in T_{\text{ex}}(e_i)} \left(\text{CheckMutates}(\text{full_ordered}, T_{\text{cvg}}(g.p_i), e^\#, T_{\text{ext}}(g.p_i)); \right.$
1277		$\left. \text{RecordRead}(\tau_v^{\text{post}}, T_{\text{cvg}}(g.p_i), e^\#, T_{\text{init}}(g.p_i), \emptyset, T_e(e_z)) \right)$
1278	Non-atomic <i>non-read-only</i>	$\vdots_{e^\# \in T_{\text{ex}}(e_i)} \left(\text{CheckMutates}(\tau_v^{\text{pre}}, T_{\text{cvg}}(g.p_i), e^\#, T_{\text{ext}}(g.p_i)); \right.$
1279		$\text{CheckReads}(\text{temporal_ordered}, T_{\text{cvg}}(g.p_i), e^\#, T_{\text{ext}}(g.p_i));$
1280		$\text{ClearReads}(e^\#);$
1281		$\text{ClearMutates}(e^\#);$
1282		$\left. \text{RecordMutate}(\tau_v^{\text{post}}, T_{\text{cvg}}(g.p_i), e^\#, T_{\text{init}}(g.p_i), \emptyset, T_e(e_z)) \right)$
1283		where τ_v^{pre} = temporal_ordered if $g.p_i$ is write-only, else full_ordered.
1284	Atomic	$\vdots_{e^\# \in T_{\text{ex}}(e_i)} \left(\text{CheckMutates}(\text{atomic_only}, T_{\text{cvg}}(g.p_i), e^\#, T_{\text{ext}}(g.p_i)); \right.$
1285		$\text{CheckReads}(\text{temporal_ordered}, T_{\text{cvg}}(g.p_i), e^\#, T_{\text{ext}}(g.p_i));$
1286		$\text{ClearReads}(e^\#); (\text{note lack of ClearMutates})$
1287		$\left. \text{RecordMutate}(\tau_v^{\text{post}}, T_{\text{cvg}}(g.p_i), e^\#, T_{\text{init}}(g.p_i), T_{\text{atom}}(g.p_i), T_e(e_z)) \right)$
1288		
1289		
1290		
1291		

Fig. 19. Argument conversion $T_{\text{arg}}(g.p_i, e_i, e_z)$. τ_v^{post} = unordered if $T_{\text{ooo}}(g.p_i)$, else full_ordered.

1292	Type	Definition
1293	$T_{\text{ext}} : \text{Expr} \rightarrow \mathcal{P}(\text{QualTL})$	$T_{\text{ext}}(e) \triangleq \{ \tau_q \in \text{QualTL} \mid \tau_q \in e.\text{ext_qual_tl} \}.$
1294	$T_{\text{atom}} : \text{Expr} \rightarrow \mathcal{P}(\text{QualTL})$	$T_{\text{atom}}(e) \triangleq \{ \tau_q \in \text{QualTL} \mid \tau_q \in e.\text{atomic_qual_tl} \}.$
1295	$T_{\text{init}} : \text{Expr} \rightarrow \text{QualTL}$	$T_{\text{init}}(e) \triangleq e.\text{initial_qual_tl}.$
1296	$T_{\text{ooo}} : \text{Expr} \rightarrow \text{Bool}$	$T_{\text{ooo}}(e) \triangleq e.\text{out_of_order}$
1297	$T_{\text{cvg}} : \text{Expr} \rightarrow \text{Bool}$	$T_{\text{cvg}}(e) \triangleq e.\text{convergent}$
1298		
1299		
1300		
1301		

Fig. 20. Helper functions used by Fig. 19 argument conversion.

$$\begin{array}{c}
 \langle c_{\text{lo}}, \sigma \rangle \Downarrow_{\mathbb{Z}} m \quad \langle c_{\text{hi}}, \sigma \rangle \Downarrow_{\mathbb{Z}} n \quad m < n \quad \langle s, i, \sigma[y \mapsto m], \rho \rangle \Downarrow i', \sigma', \rho' \\
 \langle \text{for } y \text{ in } (m+1) \dots n \text{ do } s^{\#}, i', \sigma', \rho' \rangle \Downarrow i'', \sigma'', \rho'' \\
 \hline
 \langle \text{for } y \text{ in loop}(c_{\text{lo}}, c_{\text{hi}}) \text{ do } s^{\#}, i, \sigma, \rho \rangle \Downarrow i'', \sigma'', \rho'' \quad \text{LoopSTEP}
 \end{array}$$

$$\frac{\langle c_{\text{lo}}, \sigma \rangle \Downarrow_{\mathbb{Z}} m \quad \langle c_{\text{hi}}, \sigma \rangle \Downarrow_{\mathbb{Z}} n \quad m \geq n}{\langle \text{for } y \text{ in loop}(c_{\text{lo}}, c_{\text{hi}}) \text{ do } s^{\#}, i, \sigma, \rho \rangle \Downarrow i, \sigma, \rho} \quad \text{LoopDONE}$$

$$\frac{\langle s_1^{\#}, i, \sigma, \rho \rangle \Downarrow i', \sigma', \rho' \quad \langle s_2^{\#}, i', \sigma', \rho' \rangle \Downarrow i'', \sigma'', \rho''}{\langle s_1^{\#}; s_2^{\#}, i, \sigma, \rho \rangle \Downarrow i'', \sigma'', \rho''} \quad \text{SEQ} \quad \frac{i' = i + 1}{\langle \text{InctaskID}, i, \sigma, \rho \rangle \Downarrow i', \sigma, \rho} \quad \text{INCTASKID}$$

$$\frac{\langle b, \sigma \rangle \Downarrow_{\text{Bool}} \text{true} \quad \langle s^{\#}, i, \sigma, \rho \rangle \Downarrow i', \sigma', \rho'}{\langle \text{if } b \text{ then } s^{\#}, i, \sigma, \rho \rangle \Downarrow i', \sigma', \rho'} \quad \text{IF-TRUE} \quad \frac{\langle b, \sigma \rangle \Downarrow_{\text{Bool}} \text{false}}{\langle \text{if } b \text{ then } s^{\#}, i, \sigma, \rho \rangle \Downarrow i, \sigma, \rho} \quad \text{IF-FALSE}$$

Fig. 21. Big-step semantics for a loop, sequencing, an explicit task-ID increment, and a guard.

1324	$c^* = (c_1, \dots, c_k) \quad \langle c_i, \sigma \rangle \Downarrow_{\mathbb{Z}} n_i \text{ for } i = 1..k$
1325	$I = \{ (v_1, \dots, v_k) \mid 0 \leq v_i < n_i \} \quad \rho' = \rho[(x, \mathbf{n}) \mapsto (\emptyset, \emptyset, (0, 0))]_{\mathbf{n} \in I}$ ALLOC
1326	$\langle \text{Alloc}(x[c^*]), \iota, \sigma, \rho \rangle \Downarrow \iota, \sigma, \rho'$
1327	
1328	$\langle e^\#, \sigma \rangle \Downarrow_{\text{Acc}} W_{e^\#} \quad \rho' = \rho[(x, \mathbf{n}) \mapsto (\emptyset, \rho(x, \mathbf{n}).m, \rho(x, \mathbf{n}).b)]_{(x, \mathbf{n}) \in W_{e^\#}}$ CLEARREADS
1329	$\langle \text{ClearReads}(e^\#), \iota, \sigma, \rho \rangle \Downarrow \iota, \sigma, \rho'$
1330	
1331	$\langle e^\#, \sigma \rangle \Downarrow_{\text{Acc}} W_{e^\#} \quad \rho' = \rho[(x, \mathbf{n}) \mapsto (\rho(x, \mathbf{n}).r, \emptyset, \rho(x, \mathbf{n}).b)]_{(x, \mathbf{n}) \in W_{e^\#}}$ CLEARMUTATES
1332	$\langle \text{ClearMutates}(e^\#), \iota, \sigma, \rho \rangle \Downarrow \iota, \sigma, \rho'$
1333	
1334	
1335	$\langle e^\#, \sigma \rangle \Downarrow_{\text{Acc}} W_{e^\#} \quad \langle e_z^\#, \sigma \rangle \Downarrow_{\text{Acc}} W_{e_z^\#}$
1336	$\rho' = \rho[(x, \mathbf{n}) \mapsto (\rho(x, \mathbf{n}).r \cup \mathcal{R}(\tau_v, t, \tau_q, \tau_q^*, W_{e_z^\#}, \rho, g_{s^\#}(\sigma, \iota)), \rho(x, \mathbf{n}).m, \rho(x, \mathbf{n}).b)]_{(x, \mathbf{n}) \in W_{e^\#}}$ RECORDREAD
1337	$\langle \text{RecordRead}(\tau_v, t, e^\#, \tau_q, \tau_q^*, e_z^\#), \iota, \sigma, \rho \rangle \Downarrow \iota, \sigma, \rho'$
1338	
1339	$\langle e^\#, \sigma \rangle \Downarrow_{\text{Acc}} W_{e^\#} \quad \langle e_z^\#, \sigma \rangle \Downarrow_{\text{Acc}} W_{e_z^\#}$
1340	$\rho' = \rho[(x, \mathbf{n}) \mapsto (\rho(x, \mathbf{n}).r, \rho(x, \mathbf{n}).m \cup \mathcal{R}(\tau_v, t, \tau_q, \tau_q^*, W_{e_z^\#}, \rho, g_{s^\#}(\sigma, \iota)), \rho(x, \mathbf{n}).b)]_{(x, \mathbf{n}) \in W_{e^\#}}$ RECORDMUTATE
1341	$\langle \text{RecordMutate}(\tau_v, t, e^\#, \tau_q, \tau_q^*, e_z^\#), \iota, \sigma, \rho \rangle \Downarrow \iota, \sigma, \rho'$
1342	
1343	$\lambda = (r \mapsto \mathcal{A}(r, g_{s^\#}(\sigma, \iota), \tau_q^{\text{full}*}, \tau_q^{\text{temp}*}) \text{ if } \mathcal{W}(t, g_{s^\#}(\sigma, \iota), \tau_q^{\text{pre}*}, r) \text{ else } r)$ FENCE
1344	$\langle \text{Fence}(t, \tau_q^{\text{pre}*}, \tau_q^{\text{full}*}, \tau_q^{\text{temp}*}), \iota, \sigma, \rho \rangle \Downarrow \iota, \sigma, \text{lift}(\rho, \lambda)$
1345	
1346	
1347	$\langle \langle e_{z1}^\#, \dots, e_{zk}^\# \rangle, \sigma \rangle \Downarrow_{\text{Acc}} W_{e_{z1}^\#}, \dots, W_{e_{zk}^\#} \quad \{(z, \mathbf{n})\} = \bigcap_{i=1}^k W_{e_{zi}^\#} \quad \mathbf{W} = \bigcup_{i=1}^k W_{e_{zi}^\#}$
1348	
1349	$\lambda = (r \mapsto (r.q, r.f, r.p[(z, \mathbf{n}) \mapsto r.p(z, \mathbf{n}) \cup \{a\}]_{z, \mathbf{n} \in \mathbf{W}}^{(a_\sim) = \rho(z, \mathbf{n})}) \text{ if } \mathcal{W}(t, g_{s^\#}(\sigma, \iota), \tau_q^{\text{pre}*}, r) \text{ else } r)$
1350	$\rho' = \text{lift}(\rho, \lambda) \quad (R', M', (a', w')) = \rho'(z, \mathbf{n}) \quad \rho'' = \rho'[(z, \mathbf{n}) \mapsto (R', M', (a' + 1, w'))]$ ARRIVE
1351	$\langle \text{Arrive}(t, \tau_q^{\text{pre}*}, e_z^{\#*}), \iota, \sigma, \rho \rangle \Downarrow \iota, \sigma, \rho''$
1352	
1353	$\langle e_z^\#, \sigma \rangle \Downarrow_{\text{Acc}} \{(z, \mathbf{n})\} \quad (a, w) = \rho(z, \mathbf{n}).b \quad \text{Max} \triangleq \text{if } n \geq 0 \text{ then } a - (n + 1) \text{ else } w + n + 1$
1354	$\text{New} \triangleq \text{if } n \geq 0 \text{ then } \max(w, \text{Max} + 1) \text{ else } w + 1$
1355	
1356	$\lambda = (r \mapsto \mathcal{A}(r, g_{s^\#}(\rho), \tau_q^{\text{full}*}, \tau_q^{\text{temp}*}) \text{ if } \exists i. i \leq \text{Max} \wedge i \in r.p(z, \mathbf{n}) \text{ else } r)$
1357	$\rho' = \text{lift}(\rho, \lambda) \quad (R', M', (a', _) = \rho'(z, \mathbf{n}) \quad \rho'' = \rho'[(z, \mathbf{n}) \mapsto (R', M', (a', \text{New}))]$ AWAIT
1358	$\langle \text{Await}(e_z^\#, \tau_q^{\text{full}*}, \tau_q^{\text{temp}*}, n), \iota, \sigma, \rho \rangle \Downarrow \iota, \sigma, \rho''$
1359	
1360	Fig. 22. The big-step operational semantics for Abstract Machine statements with sync environment updates.
1361	
1362	
1363	
1364	
1365	
1366	
1367	
1368	
1369	
1370	
1371	
1372	